HASIL CEK_60201248 JURNAL 2

by Cek_60201248 60201248

Submission date: 09-Apr-2021 09:10AM (UTC+0700)
Submission ID: 1554175863
File name: CEK_60201248_jurnal_2_saya.pdf (6.69M)
Word count: 19385
Character count: 95537

Journal of Materials Chemistry B

REVIEW

View Article Online
View Journal | View Issue

Cite this: J. Mater. Chem. B, 2017, 5, 6193

Synthetic strategies and biomedical applications of I–III–VI ternary quantum dots

Wubshet Mekonnen Girma,[a] Mochamad Zakki Fahmi,[b] Adi Permadi,[a] Mulu Alemayehu Abate[a] and Jia-Yaw Chang*[a]

Received 27th April 2017,
Accepted 29th June 2017

DOI: 10.1039/c7tb01156c

rsc.li/materials-b

Surface modified and bioconjugated quantum dots (QDs) are of central importance in biomedical applications. In this regard, particularly I–III–VI QDs are of specific interest for biosensors, multimodal imaging, chemotherapy and for phototherapy in theranostic applications. Surface modification allows management of the physico-chemical properties, biocompatibility, and pharmacological properties. This review is anticipated to provide an introduction to new researchers about I–III–VI type QDs relating to their synthesis, optical properties, surface modification, bioconjugation, and their applications in biosensors, biological imaging, drug delivery, photothermal therapy and photodynamic therapy. We also highlight introducing magnetic metals and nanoparticles to these QDs for multimodal imaging applications and have addressed toxicity related issues. Finally, we summarize the results obtained and give a short outlook on future directions of I–III–VI based QDs for biomedical applications.

1. Introduction

Quantum dots (QDs) are semiconductor nanocrystals with size dependent optical and electronic properties which are composed of inorganic core materials with an organic outer layer of capping ligands. Colloidal QDs are characterised by their structures and band gap energies (less than 4 eV) between the valance band (VB) and conduction band (CB). The electronic properties differ from the bulk crystals since, as the size decreases, the band gap energy shifts to higher energy (shorter wavelength). The development of different synthesis methods and size dependant optical properties in the quantum confinement region has tremendous impact on the advancements of a wide range of applications including solar cells, photocatalysis, biosensing, drug delivery, detection and bioimaging.

To become biologically applicable, QDs should be biocompatible and ideally absorb in the near infrared region (NIR). Such small fluorescent nanocrystals have recently become a major focus in biological and medical sciences which enable high

[a] Department of Chemical Engineering, National Taiwan University of Science and Technology, 43, Section 4, Keelung Road, Taipei, 10607, Taiwan, Republic of China. E-mail: jychang@mail.ntust.edu.tw; Fax: +886-2-27376644; Tel: +886-2-27303636
[b] Department of Chemistry, Airlangga University, Surabaya 60115, Indonesia

Wubshet Mekonnen Girma

Wubshet Mekonnen Girma received his BSc degree in Applied Chemistry, from University of Gondar, Ethiopia in 2010 and his MSc degree in Inorganic Chemistry from Addis Ababa University, Ethiopia in 2013. Currently he is a PhD candidate in the Departments of Chemical Engineering, National Taiwan university of Science and Technology. His research fields focus on ternary copper based nanomaterials for theranostic application under the supervision of Prof. Jia-Yaw Chang.

Mochamad Zakki Fahmi

Mochamad Zakki Fahmi received his PhD at Chemical Engineering, National Taiwan University of Science and Technology in 2014 under the supervision of Prof. Jia-Yaw Chang. Currently, he is Assistant Professor at Department of Chemistry, Universitas Airlangga, Indonesia. His research interests were focused on developing synthesis and modification of polymers and nanomaterials for bioapplication.

sensitivity imaging of cells, tissues and biomolecules. Such QDs are of pronounced interest for advanced studies in a variety of applications such as light emitting diodes,[1–5] light-harvesting systems,[6] lasers and sensors,[7] and biomedical labelling.[8–10]

The most intensively studied QDs are the II–VI, III–V and IV–VI binary semiconductors such as CdS, CdSe, CdTe, PbS and PbSe and their alloys, and they have been manly studied in the form of size- and shape-controlled NCs during the past decade.[11–13]

In comparison to the binary QDs, ternary I–III–VI (I = Cu, Ag; III = In, Sn, Ga, Al and VI = S, Se, Te *etc.*) chalcopyrite compounds, are composed of less toxic elements (free from Cd, Hg *etc.*), and are considered as promising candidates to develop eco-friendly QDs.

Although many reviews have been published on the use of QDs in biology and biomedical fields,[14–21] in this perspective, mainly we summarize the different kinds of I–III–VI QDs (such as $CuInS_2$ (CIS), $CuInSe_2$ (CISe), $AgInS_2$ (AIS), $AgInSe_2$ (AISe)), which have been applied in biosensors, imaging, drug delivery, photothermal therapy (PTT) and photodynamic therapy (PDT). Most of the chosen reference papers in this review are related to ternary QDs applied to biological applications. Moreover, a few representative papers not related to biological application are cited to show different synthesis approaches and optical properties of I–III–VI QDs. We hope to add some value to this review by revealing many practical aspects of synthesis approach, tuning optical properties, surface functionalization and uses as biosensors, in dual modal imaging, drug delivery and light-activated therapy, that are not clearly explained and discussed in the general literature. We begin by discussing the quantum confinement effect, and then discuss optical properties of ternary QDs and core/shell systems, doping heteroatoms, different synthesis approaches, phase transfer strategies, and then functionalization and bioconjugation. Finally, the biological application of I–III–VI QDs, specifically CIS, CISe, AIS and AISe QDs in biosensors, imaging, drug delivery, PTT and PDT, with toxicity related issues are discussed. Each section provides a brief historical outline, which is important to understand the follow up discussion in most recent progresses in the field. We will attempt to guide new researchers in terms of the advantages and disadvantages of every method in terms of physical and chemical parameters, the choice of synthetic routes and phase transfer strategies which leads to biocompatible QDs with high fluorescent intensity, to serve as excellent candidates for a number of *in vivo* and *in vitro* studies.

Adi Permadi

Adi Permadi received his BSc degree in Chemical Engineering from Gadjah Mada University, Indonesia in 2007 and his MEng degree in Chemical Engineering from Bandung Institute of Technology, Indonesia in 2010. Currently he is a PhD candidate in the Departments of Chemical Engineering, National Taiwan University of Science and Technology, Taiwan. His research focus, under the supervision of Prof. Jia-Yaw Chang, is on ternary quantum dots for staining cancer cells.

2. Overview of I–III–VI QDs

2.1 Summary on the uses of I–III–VI QDs

Studies focusing on I–III–VI QDs are growing in number and attracting researchers from different areas. (i) Diode laser applications ranging from their physics of operation to device

Mulu Alemayehu Abate

Mulu Alemayehu Abate received his master's degree in Inorganic Chemistry from Arba-Minch University, Ethiopia in 2013. Currently, he is a PhD candidate under the supervision of Prof. Jia-Yaw Chang at National Taiwan University of Science and Technology department of Chemical Engineering, Taiwan. His recent research mainly focuses on quantum dot sensitized solar cells.

Jia-Yaw Chang

Jia-Yaw Chang received his PhD in Chemistry from National Tsing Hua University in 2004 under the supervision of Prof. Yong-Chien Ling. He was a visiting researcher in the laboratory of Prof. Weihong Tan at the University of Florida in 2003. From 2004 to 2009, he was a research scientist and a project leader at Industrial Technology Research Institute. He joined National Taiwan University of Science and Technology in 2009 as an Assistant Professor and became a Professor in 2015. His research interests include the synthesis and functionalization of nanomaterials in the areas of energy conversion, drug delivery, light-activated therapy, and bioimaging applications.

engineering. (ii) Synthetic studies exploring different chemical compositions and spectroscopic aspects. (iii) Developing novel devices for the conversion of solar to electrical energy. (iv) Their applications in biosensing, imaging phototherapy and chemotherapy of interest to biologists and medical science. Such research could lead to a great contribution towards potential improvements of these semiconductor materials in the future.

Biological applications with highly fluorescent and photostable QDs requires QDs with NIR emission, small size, water solubility and nontoxicity. Ternary chalcopyrite QDs can achieve these requirements and hence are good candidates for such applications. Particle size and stoichiometric compositions variations allow to tune the emission wavelength in the window for biological applications from 600–900 nm.

2.2 Quantum confinement, optical properties, and core/shell structure of I–III–VI QDs

QDs are constructed from semiconductor materials and their optical properties are greatly affected by the interactions among electrons, holes and surroundings. Absorption of photons in QDs is observed when the energy difference of CB and VB is lower than the energy of absorbance. At this time, VB electrons are excited to the CB leaving a 'hole'. The average physical distance between conduction electrons and valence holes is defined as the exciton Bohr radius (α_B). Once the electron is excited to CB, it falls back down across the band gap towards the VB. At this time electromagnetic radiation energy is lost and the corresponding wavelength is emitted. Increase in band gap energy is related to size, composition and shape of quantum confinement. This is due to quantum confinement and will happen when the QDs is in the size range of the exciton Bohr radius.[22,23] Quantum confinement in QDs is defined in terms of decreasing QDs size and widening the band gap. In the case of QDs the energy between VB and CB is discrete due to quantum effects, and the energy band gap increases as the QDs size decreases, which affects the properties. There are two major effects which varies the QDs size. First, the surface atom ratio in the QDs which contribute to the free energy and is accountable for changes in thermodynamic properties. Second, intrinsic properties of QDs which are transformed by quantum size effects: optical and electrical properties of QDs show strong variations with size. The most interesting properties of QDs are their tunable optical and electrical properties as a function of particle size (Fig. 1).[24] The intrinsic electron and hole carriers lead to increased band gap energy and to the splitting of continuous energy bands in the discrete energy levels in spatial confinement. This absorption and emission properties of QDs are particularly important for biological imaging and therapy.[25]

Ternary I–III–VI materials display direct band gap in the visible region with band gaps of 1.05 eV (CISe) and 1.5 eV (CIS),[5,26,27] 1.87 eV (AIS) and 1.2 eV (AISe).[28,29] Ternary I–III–VI QDs also have a large optical absorption coefficient for CIS ($\alpha > 10^5$ cm^{-1}),[30] and high photostability (excited state lifetime).[8] In addition to this, these QDs have been reported to display high quantum yield (QY),[31–34] long luminescence decay time and a large Stokes shift (wide energy separation between absorption and emission maxima).[8,35,36]

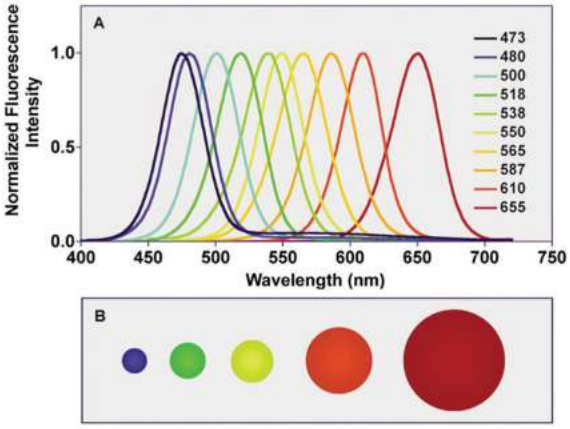

Fig. 1 (A) Size dependent fluorescence spectra of quantum dots and (B) different relative particle sizes with diameters between 2.1–7.5 nm. (Reproduced from ref. 24 with permission from the Royal Society of Chemistry.)

Moreover, composition variation consequences of I–III–VI QDs can directly tune the optical properties. The presence of different atoms in their composition enables tuning of the absorption spectra. Several reports show that the non-stoichiometry of ternary I–III–VI QDs could be controlled by the molar ratios of precursors.[8,37,38] The tunable emission is a important property of I–III–VI QDs which attracts significant research in biomedical applications, since fluorescence is widely used in cell, tissue and animal experiments.

Ternary I–III–VI QDs prepared as core QDs exhibit poor PL QYs of less than 20% and are not stable to photon-irradiation. Surface coating of the QDs with materials having a large band gap is a suitable way to enhance the PL QY as well as the stability. The surface-to-volume ratio of QDs is high due to their small size, as a result surface defects on unsaturated bonds on the surface provides non-radiative decay pathways for the photocreated charge carriers. Efficient surface passivation is required to eliminate surface defects, improve the fluorescence QY and stability. Introducing Zn^{2+} or ZnS was found to lead to optimizing of optical properties of semiconductor QDs. Deng *et al.*[39] showed that increasing Zn in the AISe system led to a blue shift on PL emission, which improved QY up to 50%. Separately, Deng also investigated optical properties of AISe after hot injection with ZnS:[40] QY of AISe QDs can reach to 40% with emission tunable from 700 to 820 nm. The emission range makes these QDs suitable for biological applications.

For example, we have shown the PL QY of AIS is dependent on the ratio of the cations ([Ag]:[In]). The fluorescent emission was strongly dependent on QDs size and as the ratio of [Ag]:[In] increases the crystal growth is faster. When the concentration of indium is increased this reduces nonradiative recombination.[41] Furthermore, recently Jara *et al.*[42] reported that copper deficient CIS QDs shows two independent optical transition absorptions, related to excitonic and Cu-related sub band gap

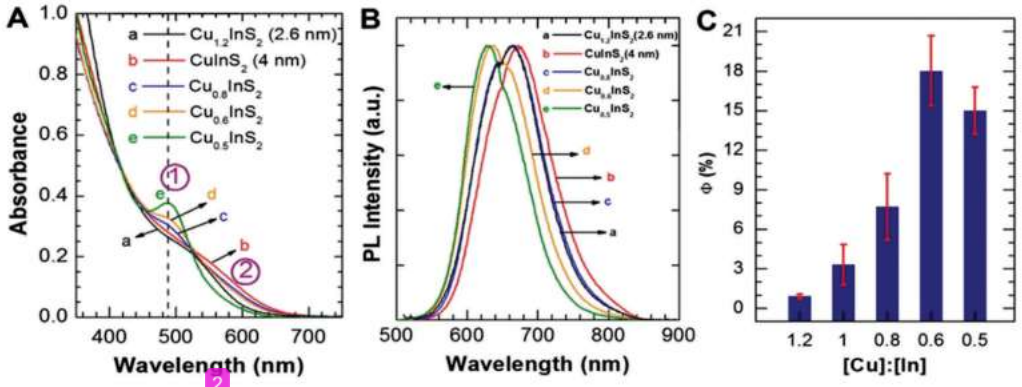

Fig. 2 (A) Different [Cu]:[In] Cu_xInS_2 QDs absorption spectra, (B) emission spectra and (C) emission quantum yield. (Reproduced from ref. 42 with permission from the American Chemical Society.)

states, respectively (Fig. 2). Hence an in depth knowledge of photo-physical mechanisms will aid in controlling properties of I–III–VI QDs and result in improvement of photovoltaic, light emitting and biological performances. The band gap of QDs can be altered by lattice stress created from the lattice mismatch between the core and shell systems.[43] The shelling material should possess a larger band gap than the core to deliver effective charge carriers while the crystal structure and the lattice parameters should be close to those of the core to facilitate epitaxial-like growth on the shell. The band gaps and lattice parameters of various semiconductors usually used in shelling the core are listed in ref. 11. As illustrated in Fig. 3, core/shell systems can be type-I, type-II and quasi-type-II by reference to their band alignments valance and conduction bands of their constituent materials. In type-I (*e.g.* CdSe/ZnS, InP/ZnS, CIS/ZnS, AIS/ZnS) core/shell systems the CB of the core is lower in energy than the shell whereas the VB of the core is higher in energy than the shell. Consequently, both holes and electrons are confined within the core. Coating of core materials with wide band gap materials is usually employed to reduce nonradiative recombination which enhances PL QY and the chemical stability. For example, Li *et al.* improved the QY of CIS materials from 5–10% to 86% by adding a CdS shell.[31] In the case of type-II QDs (Fig. 3C) one of the materials has both VB and CB higher in energy than the other material. Unlike type-I QDs one of either the electron or holes is mainly confined to the core while the other is confined to the shell. In type I/II core/shell structures CdS,[44] CdSe,[45] ZnTe[46] and ZnS[47,48] are used as shell materials.

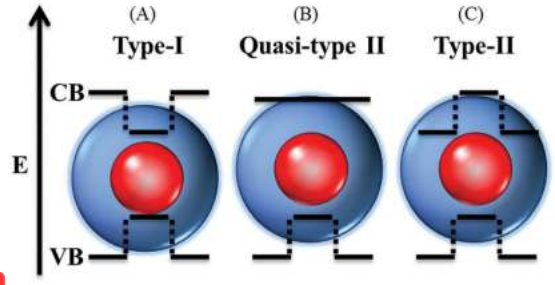

Fig. 3 Schematic band alignments: (A) type-I, (B) quasi-type-II and (C) type-II at the heterointerface between two semiconductors of core/shell QDs.

The growth of a ZnS shell layer around the surface of the core enhances the PL QY of the QDs. Most researchers choose ZnS as a shelling material due to its chemical properties. First, it has wide band gap (3.7 eV)[49] and smaller ionic radii which forms good band alignment with I–III–VI QDs. Second, its zinc blende structure allows elimination of surface trap states and avoids leakage created charge carriers in ternary core QDs. Xie *et al.*[50] demonstrated one layer of ZnS over the CIS core improved the PL QY to 30%. Jang *et al.*[51] synthesized CIS core and passivated it with two layers of ZnS shell, and the fluorescence QY was increased to 92%. The double layer shelling of ZnS leads to a remarkable blue shift from 660 to 559 nm. Speranskaya *et al.*[52] recently synthesized a core CIS core with a PL QY of 28% and after shelling with ZnS the PL QY value reached 80% with a stoichiometric ratio of Cu : In showing high photostability under UV illumination both in toluene and aqueous solutions. Surface reconstruction with ZnS provides good stability by decreasing the size of core, and leads to a shift in the absorption and emission spectra (Fig. 4).[53]

2.3 Doping heteroatoms to I–III–VI QDs

Precise and purposeful insertion of atoms into QDs in the bulk form is known as doping. Doped QDs can introduce multi-channel imaging application by introducing multiple emission peaks. For instance, zinc (Zn) doped CIS/ZnS QDs show a blue shift and can be applied for tumour targeted bioimaging.[54] Tang *et al.*[55] synthesized Zn doped AIS and comparison with a pure AIS QDs indicated the incorporation of Zn dopant leads to increased structure stability and crystallinity. Doping is also performed to introduce magnetic functionality to the QDs to afford contrast agents in MRI and multimodal imaging. Typically for these purposes paramagnetic metal ions can be doped to introduce spin–lattice relaxation and spin–spin relaxation dynamics of protons in nearby water molecules which extends

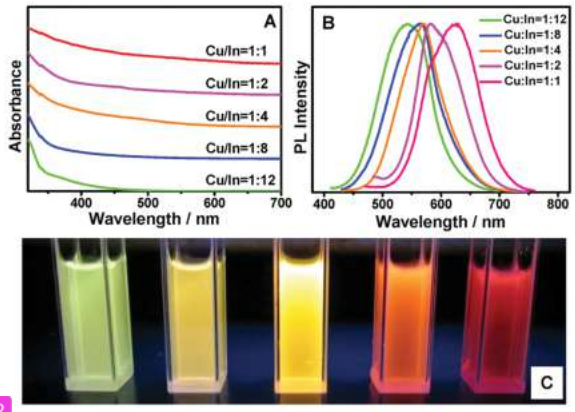

Fig. 4 (A) Absorption spectra and (B) PL spectra of CIS/ZnS QDs with different Cu/In ratios in the cores; (C) corresponding digital pictures of CIS/ZnS QDs under UV-light irradiation. (Reproduced from ref. 53 with permission from the American Chemical Society.)

the array of physical properties of the host QDs. For example Yang *et al.*[56] doped Gd^{3+} into CIS/ZnS QDs for fluorescent MR/*in vivo* imaging.

More fundamentally, doping can vary the electronic, optical and magnetic properties, and can be used to produce n-type and p-type QDs which could be applied for solar cell devices or to fabricate highly conductive NCs. Most focus has been on transition metal dopants such as Cu, Mn and Zn which can serve to tune the properties of the host QDs. In this respect, when paramagnetic dopants are introduced into the lattices of ternary QDs, escape of ions into the surrounding medium is suppressed. One should consider that several synthetic methods critically influence the doping efficiency as well as the optical properties of the host QDs. Moreover, doping to core QDs requires consideration of the "hard and soft acids and bases" (HSAB) principle; for example when considering Mn^{2+} and Zn^{2+}, Mn^{2+} has a harder nature than Zn^{2+}, hence there is a difference in solubility products which reduces their corresponding metal sulfide co-precipitation during synthesis of ternary QDs. In this regard, doping of soft acids to the ternary system may facilitate the incorporation into the lattice crystal and reaction with the anion precursor rather than hard base solvents present in the reaction media. Therefore during synthesis of doped ternary QDs it is necessary to target the acid strength of the dopant and choose appropriate ligands most specifically in aqueous phase synthesis approaches.

3. Synthesis and modification of I–III–VI QDs

Several researches on the synthesis of I–III–VI QDs and effective routes to highly luminescent core/shell ternary QDs have been reported.[31,57–60] Fabrication of I–III–VI QDs are adapted from the methods used in II–VI binary QDs from the literature.[61–63] During synthesis of QDs, the reaction temperature and time,[8,64] injection temperature in hot-injection methods,[65] the reactivity and the stoichiometric ratios of precursors, the solvent type used, surfactant, and pH,[66] *etc.* are important parameters to adjust the size and composition. A number of metal salts and sulfur precursors are used for the preparation of luminescent I–III–VI QDs by thermolysis in hot organic solvents.[35,64,67–69]

Difficulties faced in the synthesis of ternary QDs arises from the fact that the chemistry of I–III–VI QDs can be particularly complex given the chemical properties of the two cations. Cu^{+} and Ag^{+} are soft Lewis acids, whereas In^{3+} is a hard one; consequently, there is a difference in their reactivity towards sulfur compounds (soft Lewis bases). Unbalanced cationic precursors will lead to the formation of copper sulfides or silver sulfides and indium sulfides, rather than growth of ternary QDs. Regulating the reactivity of Cu and In precursors at the same time can be achieved by having more than one kind of capping ligands, *e.g.*, a thiol and a carboxylic acid, for controlling the reactivity of Cu^{+} and In^{3+} cations, respectively.[50,70] Also using one excess stabilizer as a solvent and ligand, *e.g.*, thiol,[31,35,71] is another alternative to reduce the cations forming side reaction products. Another strategy to avoid the problem of different reactivities is the use of single precursors containing both precursor cations, which provides the same amount of Cu and In at once, which promote the formation of CIS or CISe instead of metal sulfides.[67,72] In 2003 Castro *et al.*[67] synthesized CIS and CISe QDs through single precursors using $(PPh_3)_2CuIn(SEt)_4$ and $(PPh_3)_2CuIn(SePh)_4$ respectively. Although the particle size of CIS they synthesized is not small enough (larger than 8 nm) to exhibit quantization effects, these precursors provided a route to colloidal chalcopyrite QDs. In 2004 they modified the experimental conditions and successfully synthesized CIS QDs smaller than 4 nm size by increasing the reaction temperature.[68] Ternary QDs have enhanced significance as compared to binary QDs since they have larger Stokes shifts, enhanced PL lifetime and size tunable emissions and low toxicity. However, the PL QY is mostly less than 10%, which is not sufficient for practical use.[31,50,73] Based on these studies numerous efforts has been made to raise the PL QY; for example, Uehara *et al.*[37] enhanced the fluorescence of CIS QDs by introducing crystal defects through a highly Cu deficient composition from CIS. This enhanced fluorescence was due to large number of donor or acceptor defects required for "donor–acceptor pair recombination (DAP)" of excited charge carriers.[35,74] Hamanaka *et al.*[75] showed the decrease in PL QY in CIS QDs is associated with deep surface traps rather than DAP. These opens a way for researchers to construct efficient approaches for modifying the surface of ternary core QDs.

3.1 Nucleation and growth

The synthesis process of core/shell systems involves two steps, initial core QDs synthesis and subsequent shell growth. During growth of shells a few monolayers of a material is deposited on the surface of the core.

Basically according to the model of Lamer,[106] with colloidal systems, QDs are synthesized *via* a three-stage process (Fig. 5). In stage one, the precursor compounds are rapidly mixed with a mixture of solvents and organic ligands. The monomer concentration increases until critical supersaturation is reached.

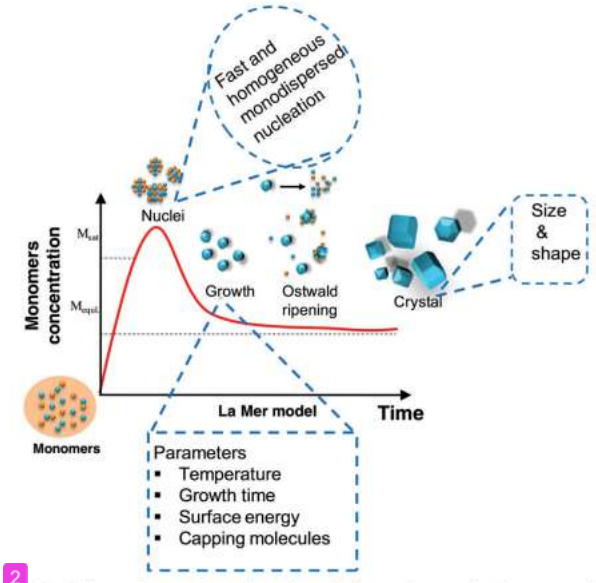

Fig. 5 Schematic representation of nucleation and growth of nanocrystals and illustration of the steps in synthesis of colloidal QDs.

At this point, seed particles precipitate spontaneously from solution (nucleation, stage 2). This is followed by a period in which the newly formed seeds capture dissolved atoms or molecules from solution, and grow to form the desired QDs until complete depletion of monomers (growth, stage 3). However, further growth of the formed QDs may occur due to Ostwald ripening, where large nanoparticles compete with small nuclei during formation. Ostwald ripening is the mechanism of growth by which smaller particles dissolve and molecular species are released for the formation of larger particles. This often leads to the dissolution of smaller particles at the expense of further growth of the larger ones. This process typically results to the formation of polydisperse samples. One can note that during the growth of the QDs there is formation of new nuclei, which may cause a spreading of the distribution of sizes of the colloidal QDs.

During synthesis of colloidal QDs the temperature plays a key role. First, an adequate amount of thermal energy is required for atoms to rearrange in ordered structures for the formation of crystals. Generally, lower reaction temperatures are required for synthesis of nanomaterials; consequently, their melting temperature depends on the thermodynamic size effects. Capping ligands also have to be considered, since they can also form complexes with the precursors used rather than binding to QDs. The capping ligands affinity to the surface and thermal stability associated with these complexes is also strongly dependent on the reaction temperature. A lower reaction temperature leads to stable complexes, lower reactivity of precursors (decreased diffusion rate) and strong binding of the ligand to surface of QDs. Nevertheless, working at higher temperature could lead to less control of size and shape or aggregated system. Consequently, use of a suitable temperature is extremely important for control of the size and shape of QDs.

The type of capping ligands is another key parameter to adjust the synthesis of QDs. Weak capping ligands cannot prevent aggregation of the forming particles while strong coordinating ligands may hinder the nucleation and/or growth of QDs.

Generally, for the synthesis of semiconductor QDs there are several methods and some of them are discussed below accordingly in terms of the solvent, reaction temperature, quality of products *etc.* Variation of metal salts and sulfur sources along with their synthesis methods, reaction temperature and applications are summarized in (Table 1) for CIS and CISe and (Table 2) for AIS and AISe QDs.

3.2 Hot injection method

The developments of colloidal chemistry enable low cost production of high quality QDs through a wet chemistry process of QD colloidal solutions which has attracted great attention. In this method, precursors and surfactants react in a high temperature reaction in the presence of stabilizers. Surfactants have a polar head group and one or more hydrophobic hydrocarbon chains. A mixture of coordinating solvents and surfactants are heated in a reactor under argon or nitrogen flow, and precursors are quickly injected in the hot solution which leads to supersaturation. The aggregation of precursors generates reactive species which induces nucleation followed by the growth of these nuclei. The size distribution of QDs is a kinetic process, and can be controlled by fast or slow injection, driven by initial supersaturation. Fast injection delivers a narrow size distribution of QDs. In this approach, formation of a new phase during precipitation involves two distinct stages; the formation of initial nuclei (crystallization) and growth. To control the growth of QDs, ligands and concentration of reactants contribute to adjust the surface energy and chemical potential of the reaction, respectively. The hot injection method produces monodispersed QDs. Organic amines and phosphines are the most widely utilized ligands in this approach. A real breakthrough come when Murray *et al.*[61] investigated the reaction mechanism for the synthesis of monodisperse CdS, CdSe and CdTe QDs by using a mixture of tri-*n*-octylphosphine (TOP) and trioctylphosphine oxide (TOPO) as high boiling point solvent/ligand. In continuation of this approach researchers successfully implemented this route to synthesize other QDs, such as CdSe and CdTe,[61] ZnSe,[107,108] PbS,[109] PbSe,[110,111] PbTe,[112,113] CIS,[114–116] CISe,[98] *etc.* Park *et al.*[117] synthesized CIS QDs having a fluorescent QY of 8% and emission peak at 645 nm *via* the hot injection approach. They added a ZnS shell by using zinc acetate for Zn source and it showed a blue shift by decreasing the size of core (Fig. 6). Often, Zn salts or ZnS are used as combining agents to the improve optical properties of the QDs. Allen *et al.*[79] recently demonstrated CISe QDs synthesis; using bis(trimethylsilyl)selenide as a chalcogenide precursor with good size control, but only the ordered vacancy chalcopyrite compounds were formed using these approach. In 2011 Park *et al.*[118] demonstrated one-pot synthesis of CISe core having emission peaks in the window of biomedical application. Latter they modified the band gap by using a ZnS passivation layer,

Table 1 Overview of experimental synthesis procedures for CIS and CISe QDs

Precursors	Synthesis method	Reaction temperature (°C)	PL emission peak (nm)	QY (%)	Material	Application	Ref.
(S_2COEt), $In(S_2COEt)_3$, EG	Heating up	196	642	—	CIS	—	76
$[P(i\text{-}But)_3]_2CuIn(SEt)_4$ or $(PPh_3)_2CuIn(SEt)_4$, DOP	Microwave	140–170	603.5–656.5	—	CIS	—	77
Cu(ac) H_2O, $InCl_3{\cdot}4H_2O$, CS_2	Solvothermal	200	835	—	CIS	—	78
CuAc, $In(OAc)_3$, DDT, ODE	Solvothermal	240	600–750	—	CIS	—	35
I, $InCl_3$, $(Me_3Si)_2Se$, OA, TOP	Hot injection	200–280	640–975	25	CIS	—	79
$Cu(S_2CNEt_2)_2$, $In(S_2C Et_2)_3$, OA, ODE	Hot injection	200	—	—	CIS	Solar cell	64
CuI, InI_3, DDT, OA, ODE	Heating up	160–240	702	5	CIS	—	37
I, $In(OAc)_3$, $ZnSt_2$, DDT, ODE	Heating up	200–270	650–830	60	CIS/ZnS	*In vivo* imaging	8
$Cu(dedc)_2$, $In(dedc)_3$, $Zn(dedc)_2$, DDT	Hot injection	120–200	—	—	CIS/ZnS	Photovoltaic and photocatalytic	80
CuI, $In(OAc)_3$, DDT, ODE	Heating up	120–200	700–850		CIS	Light emitting and solar cell	70
Cl, $InCl_3$, sulfur, OA	Solvothermal	110–170	—	—	CIS	Solar cell	81
CuI, $In(OAc)_3$, Zn(OAC), DDT, ODE	Solvothermal	180	647–664	65	CIS/ZnS	—	82
I, $In(OAc)_3$, DDT, $ZnSt_2$, MA, ODE	Heating up	110–250	645	65	CIS/ZnS	—	83
CuI, $In(OAc)_3$, $ZnSt_2$, DDT	Heating up	100–230	630–780	86	CIS	—	84
I, $In(OAc)_3$, DDT, ODE	Heating up	120–230	683	—	CIS	—	85
$Cl_2{\cdot}2H_2O$, $InCl_3{\cdot}4H_2O$, $CS(NH_2)_2$, MPA	Hydrothermal	150	660	3.3	CIS	Biomedical imaging	66
$(NO_3)_2$, $In(OAc)_3$, sulfur, $Zn(OAC)_2OA$	Hot injection	90–170	650–800	30	CIS/ZnS	*In vivo* imaging	86
CuI, $In(OAc)_3$, DDT	Solvothermal	180	654–659		CIS	White LED	5
Cl_3, $CuCl_2$, Na_2S, $Zn(OAc)_2$	Hydrothermal	100	532–655		CIS/ZnS		87
$Cl_2{\cdot}2H_2O$, $InCl_4{\cdot}4H_2O$, $Zn(OAC)_2$, DDT, ODE	Heating up	100–250	450–559	80	CIS/ZnS/ZnS	White LED	88
$Cu(NO_3)_2{\cdot}3H_2O$, $In(NO_3)_2{\cdot}5H_2O$, $Na_2S{\cdot}9H_2O$, GSH	Hydrothermal	100	654–800	—	CIS	*In vivo* imaging	89
Cl, $InCl_3$, Se powder, DPP, OA	Hot injection	100–240	735–800		CISe	Solar cells	90
I, $In(OAc)_3$, Se powder, DDT, ODE, TBP	Hot injection	200	600–850	26	CISe//ZnS	LEDs, biolabeling	91
CuI, InI_3, $(TMS)_2Se$, TOPO, HDA, $(TMS)_2S$, ethyl zinc, DDT	Hot injection	270, 130	700–900	60	CISe/ZnS	Biomedical imaging	92
CuI, $InCl_3$, Se powder, TOP, $(Zn(CH_3COO)_2)$, DA, OLA	Hot injection	200–280	619	16	CISe/ZnSe	Solar cells and LEDs	93
CuCl, $InCl_3$, TOPSe, $(LiN(SiMe_3)_2)$, $ZnEt_2$, TOPS	Hot injection	285, 320	700–1200	60	CISe/ZnSe	Bioimaging, biolabeling, and lighting applications	94
$Cu(acac)_2$, $In(acac)_3$, Se powder, TBP, DDT, source, ODE, zinc(II) oleate	Hot injection	220	750	40	$CISe_xS_{2-x}$/ZnS	Bioimaging	95
Cl, $InCl_3$, seleneourea, ODE, TOP, DDT, $Zn(OA)_2$	Heating up	140–250	700–1040	50	CISe/ZnS	Biomedical imaging	96
CuI, $(In(OAc)_3)$, Se powder, DDT, ODE, OLA	Hot injection	130, 180, 200	709		CISe/ZnS	Bioimaging	97
I, InI_3, $(Me_3Si)_2Se$, TOP, OA	Hot injection	280, 210	650–975	25	CISe	Bioimaging	98
I, $InCl_3$, Se powder, TOP, ODE	Heating up	320	838–918	25	CISe	Solar cells	99
$(acac)_2$, $In(acac)_3$, Se powder, TOP ODE, OA	Solvothermal	170, 120			CISe	Solar cells	100
Cl, $InCl_3{\cdot}4H_2O$, Se powder, OLA	Solvothermal	220, 70		15	CISe	Photo catalyst	101
powder, In powder, Se powder, DI water	Hydrothermal	180–220	863		CISe	Photovoltaic devices	102
Cl_2, $In(OH)_3$, Se powder, Gelatin	Heating up	120, 80	612–686	23.3	CISe/ZnS	LED	103
InI_3, Se powder, OLA	Hot injection	80–270		73	CISe	Photovoltaic device	104
CuI, $(In(OAc)_3)$, Se powder, $(Zn(OAc)_2)$, powder, OLA	Hot injection	180	810		CISe/ZnS	Photovoltaic device	105

EG: ethylene glycol, DOP: dioctyl phthalate, OA: oleic acid, OLA: oleylamine, TOP: trioctylphosphine, DDT: dodecanethiol, ODE: 1-octadecene, MA: myristic acid, MPA: mercaptopropionic acid, GSH: glutathione, DPP: diphenylphosphine, TBP: tributylphosphine, $(TMS)_2Se$: bis(trimethylsilyl)selenide, TOPO: trioctylphosphine oxide, HDA: hexadecylamine.

with the CISe/ZnS core/shell system showing a blue shift for bioimaging application. Post synthetic treatment of I–III–VI QDs improve the optical properties and surface states which imparts good stability. Yarema *et al.*[94] synthesized luminescent CISe by using silylamide and controlled the size of the QDs in between 3 and 5 nm by tuning the growth time, temperature, and amount of silylamide. The QDs growth temperature and time have influence on the size of particle which in turn alters the absorption and emissions of QDs. Modification with ZnS (*via* ZnS coating, Zn diffusion and alloying with ZnS) to form AIS–ZnS (ZAIS) nanostructures is often done to enhance the PL properties of AIS. For instance, Xiang *et al.*[119] have successfully prepared AIS and AZIS QDs with various stoichiometries. By varying the Ag to Zn ratio, it is observed that addition of Zn to the crystal system effects the absorption peaks that tend to blue-shift (739 to 632 nm) and their emission wavelengths move to a higher energy accordingly, showing a quite tunable emission from red to green. Noteworthy, Zn on AIS can enhance QY up to 62% and be finely adjusted in the whole visible spectrum. Torimoto *et al.*[120] also proposed a strategy for optimizing QY of AIS. In the study, AIS QDs which were prepared *via* a pyrolysis process were further coated with ZnS separately giving the highest quantum yield of *ca.* 80%. In our previous work, we tried to develop ZnS coating onto the AIS synthesis process *via* one-pot hot injection process.[121] By this simplified synthesis step, QY can be increased up to *ca.* 70%

Table 2 Overview of experimental synthesis procedures for AIS and AISe QDs

Precursor	Synthesis method	Reaction temperature (°C)	PL emission (nm)	QY (%)	Material	Application	Ref.
$AgNO_3$, $InCl_3{\cdot}4H_2O$, DDT	Hot injection	170	639–732 at specific Ag/In	62	AIS	LED	119
$AgNO_3$, $In(NO_3)_3{\cdot}xH_2O$, diethyldithiocarbamate trihydrate	Hydrothermal	60	480–700		AIS	Cellular imaging and siRNA delivery	145
$AgNO_3$, $In(NO_3)_3$, NaS_2	Hydrothermal	100	595	20	AIS	Bioimaging	146, 147
[Ag(HSal)], $InCl_3$, sulfur	Microwave	350	653	14	AIS	Ion detection, bioimaging, solar cell	150–152
$AgNO_3$, $In(Ac)_3$, sulfur	Hot injection	200	650–820		AIS	Bioimaging	153, 154
AgAc, $In(Ac)_3$, DDT	Hot injection	270, 210	670	28	AIS	Bioimaging	131, 136, 137, 155
$AgNO_3$, $InCl_3{\cdot}4H_2O$, *N*,*N*-diethyldithiocarbamate trihydrate	Heating up	180	580–750	70	AIS	Solar cell	120, 125, 156, 157
$AgNO_3$, $In(Ac)_3$, sulfur	Hot injection	130	644		AIS	LED	132
$AgNO_3$, In(stearate), DDT	Hot injection	180	580	22	AIS	Bioimaging	121, 135
$AgNO_3$, $In(Ac)_3$, DDT	Hot injection	175, 115	675	50	AIS	Solar cell	114, 130
$AgNO_3$, $In(Ac)_3$, L-cysteine	Hydrothermal	110	560	26	AIS	Bioimaging	148
AgI, InI_3, $(Me_3Si)_2Se$	Hot injection	280	650	15	AISe		98
$AgNO_3$, $In(Ac)_3$, Se powder	Hot injection	175	700–820	40	AISe	Bioimaging	40
AgAc, $In(Ac)_3$, selenourea	Heating up	250			AISe	Solar cell	126
$AgNO_3$, $In(Ac)_3$, Se powder	Hydrothermal	90	625–940	31	AISe	Bioimaging	158, 159
Ag_2O, $In(Ac)_3$, Se powder	Hot injection	230	800–1300	21	AISe	Bioimaging	39, 160
$AgNO_3$, $In(NO_3)_3$, NaHSe	Hydrothermal	100	504–585	15	AISe	Bioimaging, LED, optical coding	149, 161

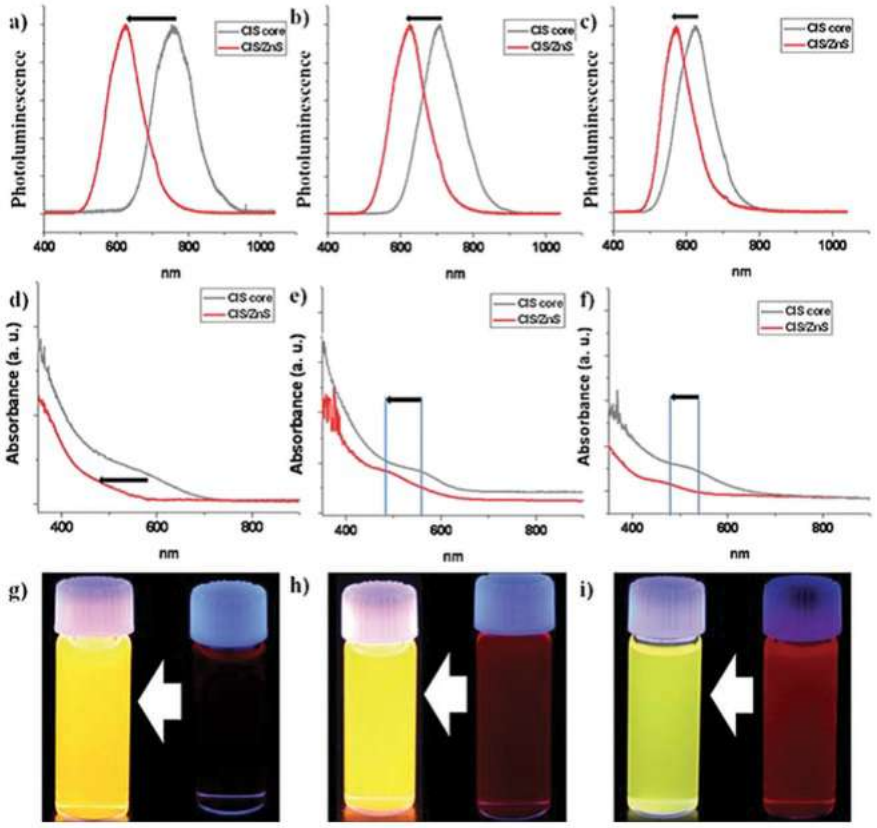

Fig. 6 The emission (a–c) and absorption (d–f) spectra of different size CIS core QDs before and after formation of a ZnS shell. (g–i) Photos of the corresponding core and core/shell under UV-irradiation. (Reproduced from ref. 117 with the permission from the Royal Society of Chemistry.)

with a slight blue shift from 570 to 520 nm. Increasing QY after ZnS coating is considered to be due to the role of ZnS as a passivating layer which could remove non-radiative recombination sites on surface of AIS.

3.3 Non-injection (heating up) approach

In this protocol the reaction solution is prepared at low temperature and subsequently heated to generate the crystallization process which leads to the QDs growth at elevated temperature. The heating up method usually consists of a high temperature decomposition of metal salts in the presence of surfactant and high boiling point solvents. The crystallization process is used to control the size distribution of the QDs and the reaction temperature depends on the reactivity of the precursors. In 2004 Cao *et al.*[122] synthesized CdS by using nucleation imitator compounds (tetraethylthiuram disulfides and 2,2′-dithiobisbenzothiazole) to isolate the nucleation and growth steps in homogeneous reaction systems. Recently in 2014 Xia *et al.*[123] synthesized CIS *via* one step by adjusting kinetic variables and coordinating molecules, such as reaction temperature, time (Fig. 7), stoichiometric ratio of precursors and stabilizing ligands. Unlike the hot injection approach, the system consists simultaneously of two different reactants before the reaction starts at a certain temperature. In this approach, instantaneous supersaturation is induced and crystallization-rate is less controllable. Due to characteristic limitations of the injection method various research groups have synthesized CIS by using the simple heating up approach.[8,35,37,70,124] As an example, Li *et al.*[31] demonstrated the influence of increased temperature on the growth of CIS QDs as indicated by an emission peak shift from 630 to 780 nm indicating increasing particle size. Increase in reaction temperature facilitates the growth of particles so introducing a degree of control. Desired sizes can be obtained after quenching the reaction by putting the flask in a water bath.

Dai *et al.* and Kameyama *et al.* was reported utilization of a non-injection pyrolysis method for the synthesis of AIS and AISe QDs.[125,126] However, even prepared with precisely stoichiometric composition, there are difficulties in obtaining QDs with single crystal structures. For instance, synthesis of AIS proposed by Dai *et al.*[125] leads to AIS QDs with tetragonal and orthorhombic crystal forms, additionally, cubic $AgIn_5S_8$ is also obtained (Fig. 8). The heating up method is particularly advantageous for large scale synthesis of QDs as large amounts of precursors in a large volume reactor can be used.

3.4 Solvothermal approach

Solvothermal synthesis is a method similar to hydrothermal synthesis, but involves organic solvents instead of water. Compared to other methods, solvothermal synthesis has several advantages. First, solvothermal conditions permit rapid convection in solution. The comparably mild environment offers conditions to form crystals with few lattice defects and allows for the precise control over the size, shape distribution, and crystallinity of nanoparticles.[127] Second, low boiling point of the used organic solvent can provide a higher reaction pressure when conducted at higher temperatures, which will contribute to the process of crystallization. Third, because of the mild temperature, special structural features of precursors can be transferred to the products so that the morphology of products can be controlled. Solvents can also provide functional groups, which can further react with the precursors or the products to synthesize novel materials.[128,129] Finally, for some reaction systems such as those including toxic starting materials, solvothermal synthesis can reduce the release of harmful vapour during the reaction. Further the trend towards to greener technologies promotes this approach, since it reduces consumption of energy and use of expensive solvents. 1-Dodecane (ODE) is widely used in preparing both ternary I–III–VI QDs combined with several ligands such as oleic acid (OA),[114,130,131] 1-hexadecylamine (HDA),[132] oleylamine (OAM),[133–135] 1-dodecanethiol (DDT),[39,40,130,136] and TOP.[98,114,131] The application of DDT in preparing CIS and AIS has advantages in terms of potency as a ligand but also as a sulfur precursor for the QDs.[121,137]

Nam *et al.*[138] synthesized CIS QDs solvothermally at a fixed temperature of 180 °C for different reaction times and the best result was at 5 h 40 min with a QY 8.8%. Solvothermally synthesized QDs are mostly hydrophobic in nature, hence for biological application and to improve the stability they have be transformed to a hydrophilic phase.

3.5 Hydrothermal approach

The principles of green chemistry attract many scientists involved in the synthesis of nanomaterials. For example, the use of non-toxic reagents and solvents, increasing the product yield, simplicity of the purification steps, minimizing the

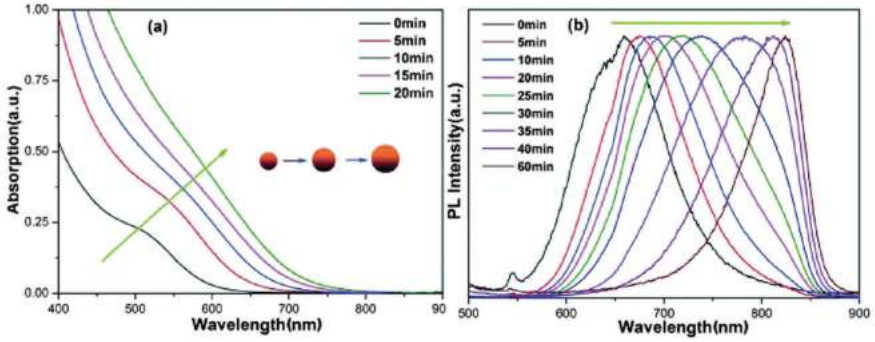

Fig. 7 (a) The absorption and (b) emission of CIS at different synthesis times for a given temperature. (Reproduced from ref. 123 with the permission from the Royal Society of Chemistry.)

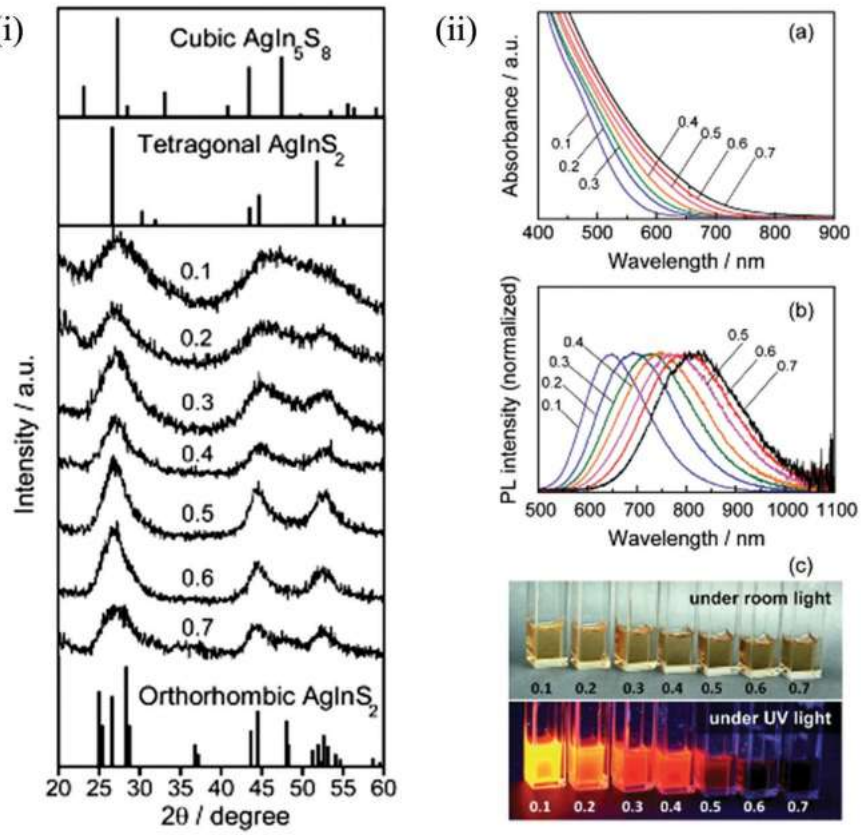

Fig. 8 (i) XRD patterns of AIS nanoparticles prepared from pyrolysis synthesis process. (ii) (a) UV spectra, (b) PL spectra and (c) photograph of AIS. (Reproduced from ref. 125 with the permission from the Royal Society of Chemistry.)

amount of organic solvents will reduce the cost of synthesis and result in reduced environmental impact.

Among the various methods of synthesis of colloidal QDs, aqueous synthesis employs environmentally friendly solvent, biocompatibility and it is not restricted to an inert atmosphere. The general synthetic approach mostly involves chemical reaction between metal precursors and surface ligands. As a metal precursor metal halides or nitrates, which are directly soluble in water, and as a sulfur source, Na_2S[53,139] and sulfourea ($CS(NH_2)_2$),[140] are mostly used. It has some distinct advantages in addition to the features of the solvothermal process. Key features of the hydrothermal approach are facile preparation, direct water-solubility, good reproducibility, low cost, and improved biocompatibility.[141,142] Rogach *et al.*[143] demonstrated the aqueous phase synthesis approach of CdTe QDs for the first time.

One-pot direct aqueous synthesis of water-soluble CIS-based QDs can be highly effective. Various hydrophilic short chain thiols (Fig. 9) are usually utilized as the ligands, such as reduced glutathione (GSH), poly acrylic acid (PAA), and thioglycolic acid (TGA) *etc.*, to prepare water-soluble CIS and CISe-based QDs. The first study on applying a hydrothermal approach for the synthesis of AIS was proposed by Luo *et al.*,[144] where they synthesized AIS QDs capped with GSH directly in water for photocatalytic application, though with low QY (15%). However, to be effectively applied in both clinical and biological applications, it is necessary to obtain high QY of QDs that are both water-dispersible and biocompatible. Based on this, several studies use a hydrothermal synthesis approach as a direct route to obtain bio-applicable QDs. Besides GSH,[27,38] some hydrophilic ligands that also act as sulfur or selenium sources, such as diethyldithiocarbamate trihydrate,[145] Na_2S,[146,147] L-cysteine,[148] NaHSe,[35,36] have been used to produce water soluble ternary system QDs which are used for biological applications. The hydrothermal method is also very flexible to alloy other elements into the AIS system resulting in improved QDs. Doping Zn^{2+} on to AIS system ($AgIn_5S_8$ QDs) was proposed by Song *et al.*[148] resulting in enhancement of QY of QDs up to 35%. This study utilized L-cysteine as a hydrophilic ligand and sulfur source. Separately, doping Ag^+ in ZISe QDs system also investigated using a hydrothermal synthesis process.[35,149]

3.6 Microwave irradiation approach

Synthesis of colloidal QDs using microwave heating is recently found to be a better approach as compared to other methods due to its numerous advantages. In microwave assisted reactions

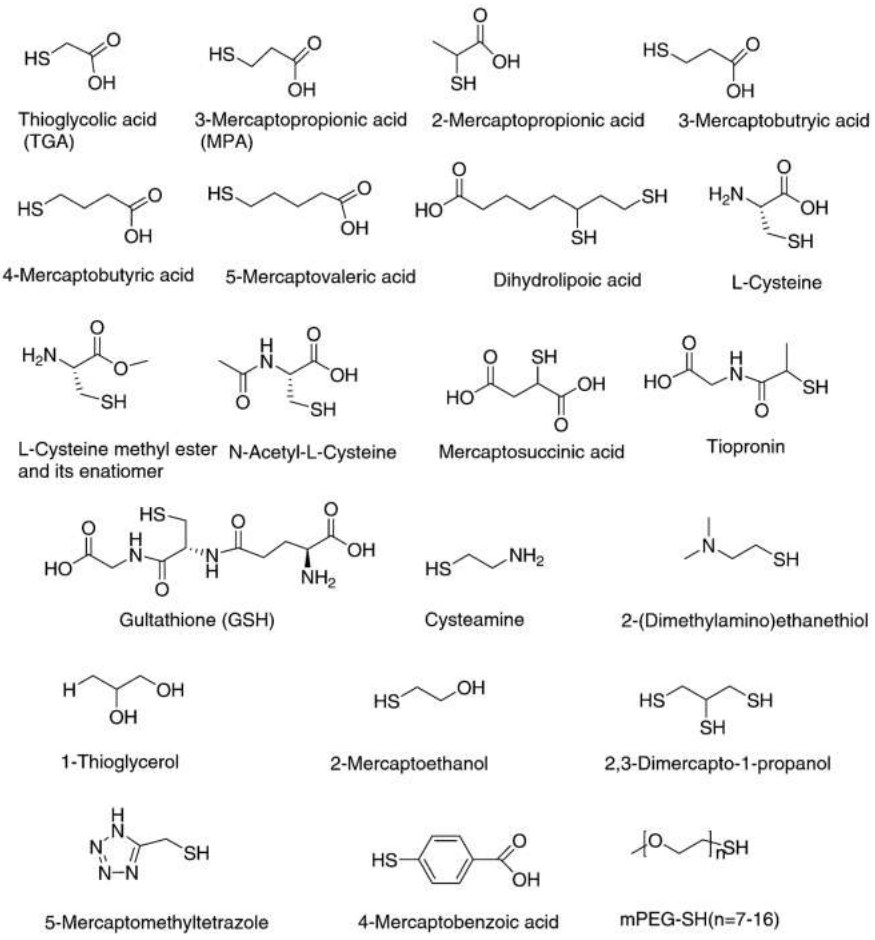

Fig. 9 Chemical structure of different possible capping ligands involved in aqueous synthesis of I–III–VI QDs.

the process is conducted at the boiling point of the solvent, at normal pressure; small particle size QDs can be prepared,[162] only short reaction time is required, purity of the product is good, and reproducibility and product yield is better.[163]

In motivation to design faster, cleaner, and economically more viable synthesis methods, many studies use microwave heating. Utilization of microwave heating in conducting chemical reactions has been adopted due to its numerous effective applications in polymer synthesis,[164] material sciences,[165] nanotechnology[162] and biochemical processes.[166] In general, sometimes extreme temperature and the rapid heating in microwave chemistry leads to faster processes. Thermodynamic and kinetic barriers of the reaction are important factors for the growth of QDs. In ordinary thermolysis reaction, conduction of black body radiation is used to drive the reaction, using the reaction vessel for transfer of energy. This can cause sharp thermal gradients in reaction conditions leading to non-uniform nucleation and particle growth.

Xiong *et al.*[152] synthesized AIS using a microwave radiation approach and further coated it with ZnS. Even using a two-step synthesis process, each process was rapid and the product showed fluorescence, low toxicity and long PL lifetimes suitable for biodetection and bioimaging. The microwave synthesis technique was also developed by Mousavi-Kamazani *et al.*[150] to produce composite Ag_2S–AIS system QDs. This study showed a clear relation between microwave power and irradiation time on the obtained nanoparticles, where higher microwave power or longer irradiation time led to increased particle size. However, most synthesis processes with the microwave approach resulted in low QY value and this problem needs to be solved.

More recently our group, synthesized Gd-doped CIS/ZnS using a facile microwave assisted approach (Fig. 10) which results in enhanced photostability applicable for both fluorescence and magnetic resonance clinical applications.[167] We summarize the differences of the above mentioned synthesis protocols according to their advantages and disadvantages in Table 3.

3.7 Phase transfer strategies and bioconjugation

QDs are mostly synthesized in nonpolar organic solvents. Since their surface is hydrophobic (aliphatic ligands such as alkyl phosphine oxides, aliphatic amines, alkyl phosphines, aliphatic carboxylic acids), we require surface coating to disperse the QDs in aqueous solution. Solubilization in aqueous systems

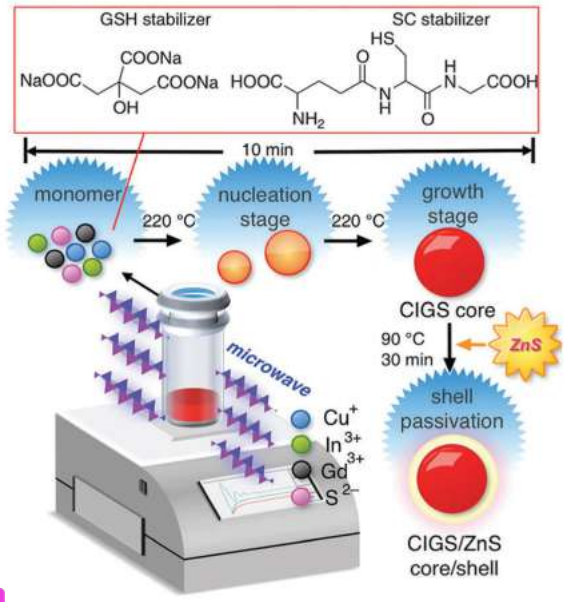

Fig. 10 Schematic of the formation of the Gd:CIS core and Gd:CIS/ZnS core/shell QDs using a microwave irradiation synthesis approach. (Reproduced from ref. 167 with permission from the Royal Society of Chemistry.)

and surface functionalization are important for many biological applications, but these processes require sophisticated surface chemistry, which is often a significant challenge. Further, QDs require ligands that modify the surface defect sites, leading to bright, photostable QDs. As shown in schematic representations in Fig. 11, various strategies have been developed to change the hydrophobic surfaces of QDs, to hydrophilic surfaces.[7,168] These strategies generally can be grouped in two types. The first protocol is ligand exchange of the original surface ligands by hydrophilic molecules.[24] The most widely used ligands are monothiolated ligands like GSH and 3-mercaptopropionic acid (MPA),[169,170] mercaptoacetic acid,[171] bidentate thiols (dihydrolipoic acid derivatives),[172] alkyl thiol terminated DNA,[173] thioalkylated oligo ethyleneglycols.[174] In this strategy, the molecules stabilizing QDs in the original first phase are changed by new stronger binding ligands and allow the transfer to the aqueous phase which also provides colloidal stability. The advantage of this method is an only small increase in the hydrodynamic radius of the QDs. This is of strong interest in QD based fluorescence resonance energy transfer (FRET) investigation[175,176] and for some biological applications which require high diffusional motilities.[177,178] Though there are limitations of this method, the stability of the thin surface ligand is often affected by local conditions, such as concentration, pH, and temperature.[172] Such conditions may prevent dispersion in the cytosol of cells. Recently, some new approaches by using similar thiol-containing molecules as L-cysteine,[179] poly(ethylene glycols)-terminated dihydrolipoic acid (PEG-DHLA)[180] have been developed for solubilization and functionalization of QDs and achieved significant *in vitro* and *in vivo* stability.[181–184] PEG-DHLA ligand has advantage to provide QDs small hydrodynamic size, low non-specific binding and high QY and shows good solubility over a wide range of pH. Li *et al.*[8] synthesized CIS/ZnS core/shell QDs initially capped with DDT surface ligand, transferred to the aqueous phase using surface ligand exchange with DHLA, and the functionalized QDs were used for *in vivo* imaging. Subramaniam *et al.*[185] have utilized MPA as a new binding ligand for dodecylamine-capped ZnS–AIS followed by polymer coating to functionalize and load siRNA. The resulting water soluble QDs has been proven to show low toxicity and to be readily applied for brain tumor staining and delivery of siRNA *in vitro*. However, a considerable issue in phase transfer *via* ligand exchange is the stability and the optical properties, in particular of QD fluorescence. In the aqueous phase, both the QDs surface and probably the thiol groups of the ligands are susceptible to oxidation. In this situation, the fluorescence QY is reduced and desorption of the capping ligands can eventually lead to aggregation.

The second strategy is based on encapsulation into a layer of amphiphilic diblock[186] or triblock copolymers,[187] phospholipid micelles,[154,188,189] silica shells,[190] dendrimers,[191] or amphiphilic polysaccharides,[192] polymer shells,[185,193–195] oligomeric phosphine coating,[196] or by phytochelatin-peptides coating,[197] or histidine-rich proteins,[198] or fatty acids.[199] This strategy was developed to overcome decreased optical properties of QDs as a limitation of the ligand exchange method. Formation of a multilayer ligand allows transfer from an organic phase to

Table 3 Summary of features of different selected synthetic methods of ternary I–III–VI QDs

Synthesis method	Advantage	Disadvantage
Hot-injection	Size control, higher quantum yield	High temperature, difficult for large scale production, use of organic solvents, use of inert atmosphere, reproducibility, reagent mixing time, cooling time
Heating	Easy large scale production, reproducibility	High temperature, use of organic solvents
Solvothermal	Size control, shape distribution, crystallinity of NCs, morphology, and reduce the release of harmful vapors	Use of organic solvents
Hydrothermal	Nontoxic solvent, cost effective, biocompatible, direct water solubility, reproducibility	Poor size control, lower PL QY
Microwave irradiation	Rapid, highly pure product, environmentally friendliness, low energy consumption, easy control of pressure and temperature profile, reproducibility, initiate rapid homogeneous nucleation, reduced crystallization time, narrow size distribution	Lower PL QY

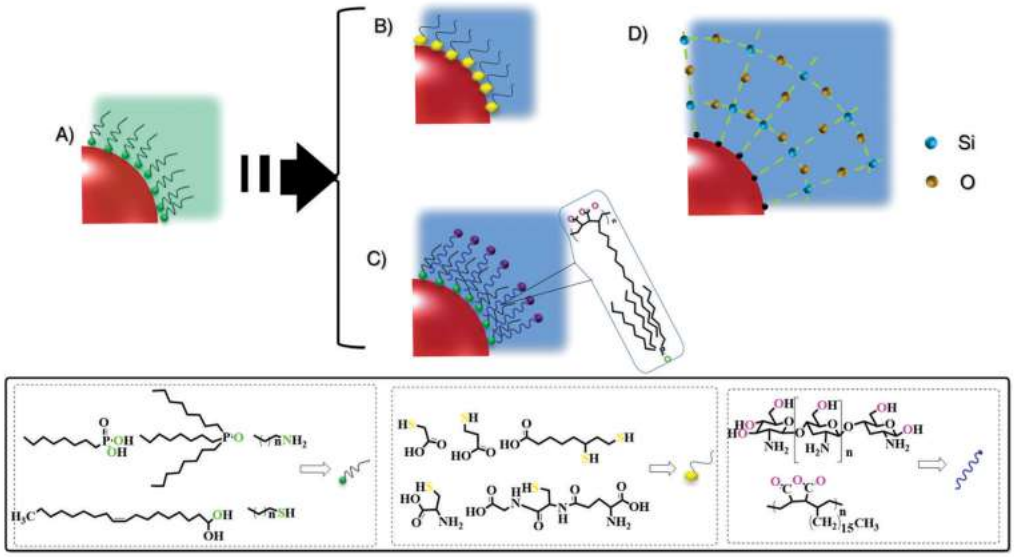

Fig. 11 Schematic representation of some phase transfer strategies: (A) QDs capped with hydrophobic ligands; (B) QD ligands exchanged with water soluble thiols; (C) QDs encapsulated with long chain polymers and chitin molecules with hydrophobic interaction; (D) QDs encapsulated with silica shells.

water phase. In this strategy, the molecules that act as phase-transfer agents have amphiphilic nature comprising of a hydrophobic and a hydrophilic part. For instance, a study on phase transfer strategy of CIS/ZnS and AIS/ZnS was conducted by Liu *et al.*[86] *via* micelle-encapsulated QD formulation. In the process, the Pluronics F127 block copolymer was used as the micelle precursor, which drives organic soluble QDs into the water phase with good optical and colloidal stability for more than 2–3 weeks. Previously, Tang *et al.*[200] also proposed Pluronics F127 as transferring polymer of AIS/ZnS and applied the transferred QDs as a staining agent on tumor cells. It is claimed that by this phase transferring process, the resulting QDs still maintain their original optical properties and were easily concentrated by slight heating to obtain desired concentrations. It was well-known that application of synthetic polymers or macromolecule materials in biological applications is favorable based on their durability and simplicity in preparation. However, in terms of safety and ease for further modification, natural polymers or biomacromolecules are the better choice. These materials offer the improvement of having the intrinsic property of environmental responsiveness as well as non-toxicity, even at high concentrations. Based on this consideration, formation of micelles was also proposed by Deng *et al.*[201] for transferring hydrophobic Zn doped AISe. The micelle was prepared *via* amphiphilic modification of chitosan by tagging with succinic anhydride. Interestingly, in this study the micelle was firstly attributed with RGD as tumor targeting agent before QD insertion (Fig. 12). In this way, the hydrophobic QDs can be effectively loaded and simultaneously transferred to water, in which the crystal structure, shape, and optical and electronic properties of the initial QDs were retained. Foda *et al.*[202] synthesized CIS/ZnS QDs in organic solvents at elevated temperature and used lipophilic silane encapsulation to make them hydrophilic for cancer cell imaging. Such encapsulated QDs have advantages, high PL efficiency and improved stability, but the thick overcoating produces large hydrodynamic diameters in the range of 20–30 nm for a 4–6 nm core/shell QD. This is limiting for biological application since they are much larger than the cellular receptors. However, the size could be reduced to the range of 17–25 nm by controlling the silica shell size and led to good biofunctionalization in cell imaging. As an alternative, Sheng *et al.*[203] proposed a phase transfer strategy of organic soluble Zn doped AIS *via* a template coating route with formatting silica layer on the QDs surface. The silica as shell of QDs can maintain the QDs from environmental damage such as oxidation and dissolution.

In our previous work, we also proposed a phase transferring strategy of organic soluble AIS/ZnS by utilizing a protein macromolecule, namely bovine serum albumin (BSA) with sonication treatment.[204] In this work, the BSA can accommodate organic soluble QDs by physical interaction with the "hydrophobic pocket" on the part of BSA covering the hydrophilic part. This situation allows the QDs to be stabilized in water. BSA is a versatile material with the ability to bind to many molecules and we showed folic acid and doxorubicin can interact with a BSA/QD composite *via* covalent and non-covalent interaction, respectively (Fig. 13). Besides large molecules, phase transfer of organic soluble AIS QDs was also performed with small molecules. We proposed a smart strategy for facile phase transfer of QDs by utilizing small amphiphilic molecules, by use of fatty acid, OAM, DDT and dodecanediol.[137] On ultrasonication treatment, the hydrocarbon part of the amphiphilic molecules can form van der Waals interactions with the hydrocarbon part of QDs, with a resulting transfer process. Using this approach, the transferred QDs still maintain their size and optical properties.

Recently several reviews on methods of synthesis, water solubilization and functionalization and applications of QDs have been published.[14,17,25,205–211] To become applicable to

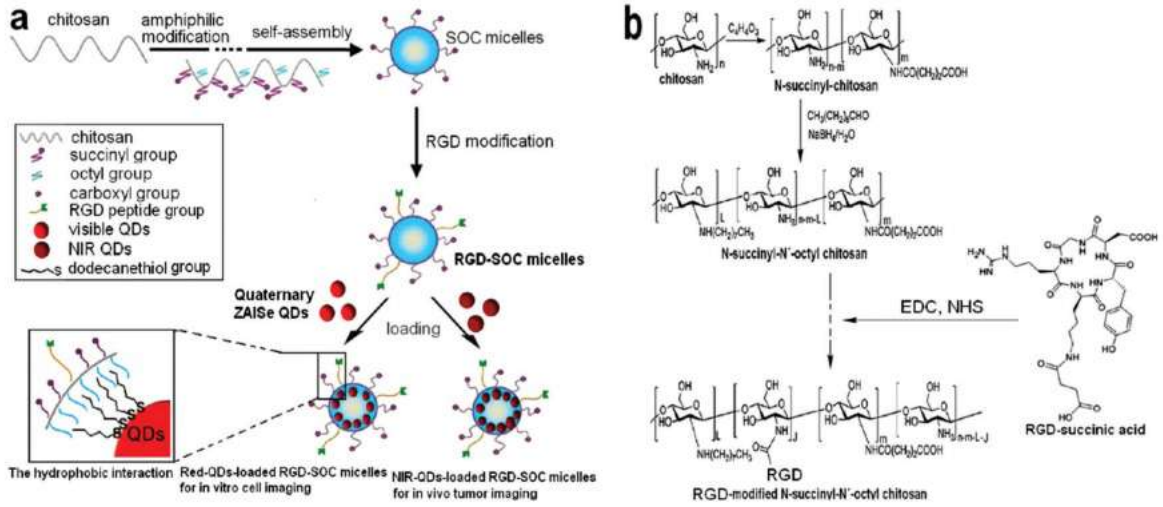

Fig. 12 (a) Overall synthetic scheme for the QD-loaded RGD-SOC micelles. (b) Synthetic scheme for RGD-modified *N*-succinyl-*N*′-octylchitosan (SOC). (Reproduced from ref. 201 with permission from the American Chemical Society.)

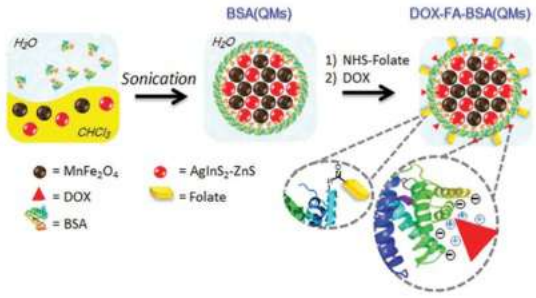

Fig. 13 Schematic route for preparing DOX–FA–BSA(QMs). (Reproduced from ref. 204 with permission from the Royal Society of Chemistry.)

biological systems certain biological molecules should be attached to the surface of QDs without changing their properties. As illustrated in the schematic representation in Fig. 14 such biological molecules are attached to the surface of QDs *via* cross linking hydrophobic surfactant molecules with reactive functional groups. Various crosslinking molecules such as 1-ethyl-3-(3-dimethylaminopropyl)carbodiimide (EDC) and 4-(*N*-maleimidomethyl)cyclohexane carboxylic acid *N*-hydroxyl succinimide ester (SMCC) are commonly used which are attached by adsorption, covalent linkage or electrostatic interaction. These are few imitations from the enormous choice of phase transfer strategies and functionalization of QDs.

To summarize, surface engineering is required to adjust the fundamental properties of QDs, to make them stable and soluble in different solvents and to create QD–biomolecule hybrids which enhances the capability of participating in biological processes. However, depending on the type of QDs and its respective biological application, the design of the surface of QDs is based on its optical properties, stability, size, solubility, biodegradability and biocompatibility. Attachments of biomolecules might lead to steric effects, alteration of enzymatic activities or molecular recognition depending of the type of biomolecules used for surface engineering of QDs. Hence, for design of specific applications, modification and improvement of bioconjugation and water-solubilization methods remain an active area of research for bioimaging, detection and therapeutics. A further area of research seeks to reduce QDs contact with normal tissue and requires specific protein binding to tumor tissue. Membrane proteins/receptors in living cells can be labeled either directly with QD–antibody or QD–ligand conjugates.

The bioconjugated surface of QDs is able to adsorb, bind and transport biomolecules such as drugs, probes and proteins. Hence they have the potential to increase the sensitivity of imaging at the cellular level including progression and treatment,[212] cancer detection,[154] as radio-and chemo-sensitizing agents,[213] as electron and X-ray contrast agents and for targeted drug delivery.[214]

4. Biomedical applications of I–III–VI QDs

In recent years, advances in nanotechnology, biology, chemistry, physics and imaging has resulted in the emergence of theranostic nanomedicines as capable agents for disease and patient-specific diagnosis and treatment. A huge number of researches have been published over the last decade and many of them have been discussed in review articles.[15,19,205,215,216] Herein we try to give an informative overview about I–II–VI QDs in different biomedical applications to provide a good starting point for interested researchers.

Due to their broad range of absorption in the NIR region and narrow emission, photophysical properties, large Stokes shift, resistance to photobleaching, and higher QYs, I–III–VI QDs are becoming more attractive for *in vitro* and *in vivo* targeting,

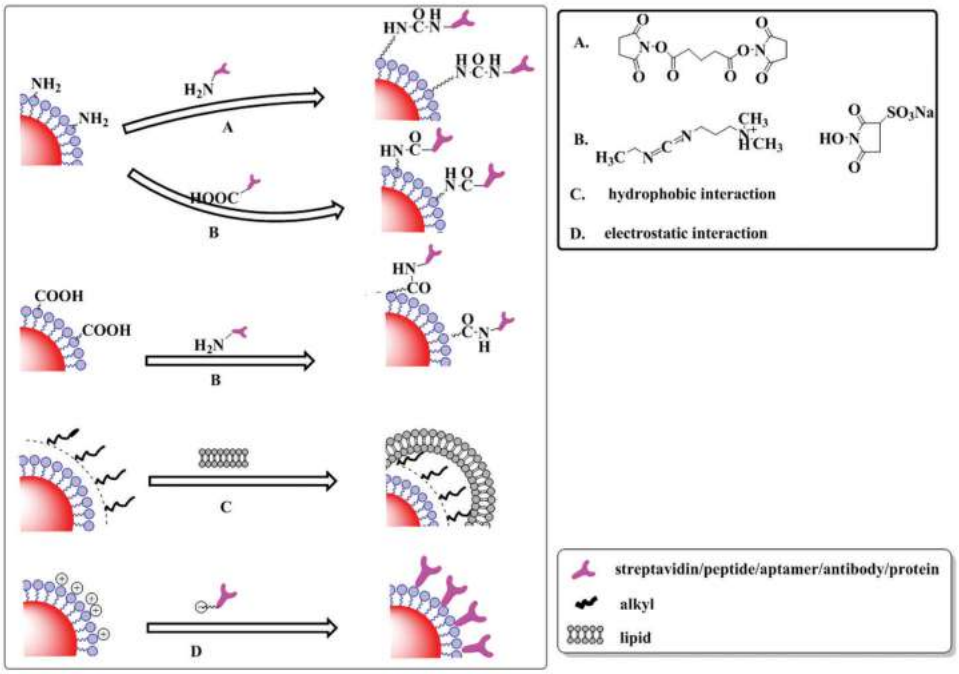

Fig. 14 Schematic presentation of QDs bioconjugation using various methods of coupling reactions and interactions.

detection/imaging and therapy of cancer cells and tissues. More specifically, functionalized I–III–VI QDs are now a component of bioengineering for biosensors, imaging, drug delivery, PTT and PDT applications. Selected biomedical applications are explained in the following sections.

4.1 Biosensors

To screen the physiological activities of cells, that lead to a range of intercellular diagnostics for diseases at the cellular level, fluorescent-based biosensors have been implemented. Among fluorescent-based biosensors, QDs display unique photo-physical and photo-chemical properties relative to organic dyes and protein fluorophores, and are thus superior fluorescence probes in sensitive biosensor applications. The developments of fluorescence and fluorescence resonance energy transfer QD-based biosensors for the detection of biomolecules such as sugars, nucleic acids, antibodies, antigens, enzymes, proteins, pathogens, small molecules, cancer biomarkers and cancer cells are widely explored.[217,218] The advances of surface engineering and bioconjugation in addition to unique properties such as narrow emission bands, photostability against photobleaching, single light source for simultaneous multi-colour excitation and single-dot sensitivity of QDs means they are a viable alternative choice for biological labelling. More specifically cadmium free I–III–VI ternary QDs are of low cost, high stability, low toxicity and high sensitivity, making them ideal candidates for bio-sensor applications. Su *et al.*[219] integrated fibrinogen with fluorescent CIS QDs as a biosensing probe for selective and sensitive detection of thrombin which is found in the blood and causes blood clotting. Their study opens a great potential for diagnosis of diseases related to coagulation abnormalities.

For clinical tests, diagnosis and other biomedical applications, immunoassay is a valuable tool. The recent developments of QD-based sensing immunoassay demonstrated multichannel detection of toxins, drug residues, chemical residues, and biomarkers. For example, Speranskaya *et al.*[220] reported the use of CIS/ZnS QDs as a fluorescent label for immunoassay quantitative analysis of the mycotoxin aflatoxin B1. Their report shows QD-based immunoassay displays enhanced sensitivity compared to enzyme-based immunoassay. Recently, Kang, Pan and their co-workers[221] reported synthesis of a gram scale polyethylenimine coated AIS QDs, and applied them for glucose detection and luminescence properties of AIS QDs used in optical imaging. The PL-intensity change of AIS QDs was used to detect glucose to recognise peroxides. Koktysh and Weiss *et al.*[222] reported detection of biotin conjugated AIS/ZnS QDs for reflectance and fluorescence measurements. Here the QDs serve as a refractive index signal amplifier and as fluorescent emitter. The other useful area of QDs application is QDs-based detection of nucleic acids. For genetic target analysis on the surface of QDs, DNA or RNA groups conjugated to form fluorescent probes. After conjugation with QDs with DNA, QDs with different emission colors can be applied to multi-plexed detection of corresponding sequences that are immobi-lized in a microarray platform.[14] Organic fluorescent labels for DNA detection have problems such as decomposition of DNA and free radical formation due to photobleaching, and further the interaction between DNA and proteins is disturbed. QDs avoid

such problems and permit color determination of orientations of a single DNA molecule.[223]

Generally, QDs conjugated with numerous anticancer antibodies can be applied for the detection of cancer biomarkers in immuno-chromatographs and immune-microchannels. For FRET-based detection, organic dye labelled strands, QDs conjugated with oligonucleic acids are prevailing platforms. QDs are greatly resistant to metabolic degradation and retain fluorescence after modification. In addition, as compared to cadmium based QDs, there is a real need to address the applications of copper and silver based ternary QDs to continue to explore better applications in live cells for the future. Evaluation of the toxicity, monodisperse preparation and specificity of QDs remain a pressing issue for the broader community interested in using QDs in live cells.

4.2 Optical imaging

Optical imaging is a fundamental tool that provides high resolution *in vitro* and *in vivo* information for biological researches. It has a number of advantages including low cost, easy portability, and potential for multiple imaging. This allows one to employ optical imaging techniques during surgery and endoscopic processes. Optical imaging is advantageous for imaging guided surgical resection of tumors and primary detection of cancer cells. For both *in vitro* and *in vivo* purposes cells or tissues can be labelled with QDs. Since copper/silver based QDs have high QY, nontoxicity, aqueous dispersibility, resistance to photobleaching, large surface area, long luminescence life times and rich surface chemistry for targeted imaging applications. I–III–VI QDs with these unique features can be applied to fluorescent imaging, multicolor imaging and in confocal imaging systems. Li *et al.*[8] synthesized luminescent CIS/ZnS QDs which were made water-dispersible through ligand-exchange using DHLA and further used as a fluorescent label for *in vivo* imaging in mice. Deng *et al.*[224] synthesized NIR-emitting AISe/ZnS QDs (with a QY of 40%) encapsulated with poly(acrylic acid)-octylamine (PAA-based) amphiphilic polymer micelles to make them water-soluble. The AISe/ZnS QDs functioned as luminescent probes for *in vitro* and *in vivo* targeted cell-imaging. For *in vitro* and *in vivo* studies RGD peptide surface modification of polymer-wrapped AISe/ZnS QDs enhanced the targeting capability of the tumor as a versatile fluorescent probe. Wang *et al.*[225] demonstrated surface modification of CIS/ZnS with trimethyl(tetradecyl)ammonium bromide (TTAB) for *in vitro* labeling of HepG2, Hela and MCF-7 cells. A fluorescence signal was observed in the cytoplasm and with increasing time of incubation CIS/ZnS–TTAB can penetrate into the nucleus. The small size of CIS/ZnS–TTAB particles of less than 10 nm and the cationic surface charge introduced by TTAB modification acted as main driving forces for the nuclear selectivity, CIS/ZnS–TTAB having ability to pass into the nucleus through the nuclear pores. Zhao, Bai and co-workers[170] reported that GSH and MPA ligand exchange can provide CIS/ZnS QDs with a better performance in solubility, stability and imaging breast tumor cells. While fluorescence of CIS/ZnS – (GSH, MPA) QDs only stays in the cytoplasm their QYs are better than for other capping ligands such as 11-mercaptoundecanoic acid (MUA), cetyltrimethylammonium bromide (CTAB) and F127 under the same conditions. Lee *et al.*[226] employed folic acid receptor as a tumor targeting ligand. The injected CIS/ZnS QDs were efficiently directed to the tumor tissue and the fluorescence signal in the tumor is highest. This means that CIS/ZnS QDs with folic acid receptor was successfully docked at the specific target. CISe/ZnS QDs conjugated with tumor targeting peptides were found to lead to strong tumor-targeting imaging probes.[97]

Up to now, there are only a handful of research articles demonstrating CIS/ZnS, CISe/ZnS, AIS/ZnS and AISe/ZnS QDs for effective use for *in vitro* and *in vivo* imaging applications.[227–229] Developments of technology and instrumentations related to different imaging modalities show there is no perfect imaging method and all suffer from limitations. Some of the limitations can be eradicated by advancements of technology, but others are a function of basic biology and chemistry, making it difficult to find a solution or even impossible in some instances. Moreover, each modality delivers information about the patient. In recent advances of QDs technology, numerous research groups are developing multifunctional or multimodal QDs that enable imaging more than a single modality, enabling to exploit the advantages of each and to obtain more information about the patient while reducing the limiting factors.

4.3 Magnetic resonance imaging (MRI)

MRI is a widely used technique in the clinic for high resolution imaging. MRI is regarded as one of leading diagnosis tools due to its unique features including its benign impact to humans and the environment since it is non-invasive with no exposure to high energy radiation, low cost, and easy implementation, high spatial resolution, and strong soft tissue contrast. Exploring the above qualities, MRI is capable for precise diagnosis of cancer. However, recently multiple modalities have been increasingly adopted and simplified coupling the complimentary abilities of different imaging modalities advanced. MRI images generally can be classified into two different imaging modes – longitudinal (T_1)-weighed and transverse (T_2) weighed images. MRI allows the imaging in deep areas of the body which is not restricted by the tissue. However, targeted contrast agents are required to achieve molecular imaging, since the sensitivity is somewhat low. Magnetic QDs have displayed great promise for targeted molecular imaging using MRI techniques. Contrast agents can accelerate the T_1 and T_2 relaxation rate in tumor cells and are used to increase the contrast between normal and cancer cells. Positive contrast agents are most particularly selected from paramagnetic metal ions containing many unpaired electrons such as Mn^{2+}, Gd^{3+} and Fe^{3+}.[56,230–232] However, negative contrast agents generally employ super-paramagnetic iron oxide nanoparticles such as Fe_2O_3 and Fe_3O_4, due to biocompatibility.[233–235]

In most MRI measurements magnetic QDs are used as contrast agents. However, to explore the advantages of absorption in the biological window and fluorescent transitions, magnetic metal doped I–III–VI type QDs are used. Researchers have already developed combinations of magnetic nanoparticles and QDs for

MRI. In work by Lin *et al.*[236] CIS–$Zn_{1-x}Mn_xS$ QDs were prepared by doping Mn and used as an optical and T_1 weighted MRI contrast agent. The encapsulation of CTAB solution aids magnetic QDs solubility in water. The results showed that fluorescence of human pancreatic cancer cell line BXPC-3 was observed clearly by confocal microscopy and were imaged by MRI. Furthermore, the feasibility of Gd-labeled Fe_3O_4 and CIS QDs conjugated with arginine-glycine-aspartic acid (RGD) was investigated by Shen *et al.*[237] Silica coating was then used to modify the $CuInS_2$ and Fe_3O_4 surface to achieve water dispersibility. Subsequently, the conjugation of Gd–diethylenetriaminepentaacetic acid (Gd–DTPA) and RGD peptides to the modified QDs@SiO_2 led to Fe_3O_4/CIS@SiO_2 (Gd–DTPA)–RGD nanoparticles. The ability of such multimodal probes for *in vitro* and *in vivo* human pancreatic cancer BXPC-3 cells was observed. The result showed that the fluorescence emission from QDs was bright and a significant signal was also detected in MRI targeted T_1 and T_2 signals, leading to enhanced effects for the treatment of cancer cells. Ding *et al.*[238] synthesized PEGylated CIS@ZnS:Mn QDs which were applied for *in vivo* fluorescence and MR imaging. Biodistribution of injected QDs in the mouse main organs such as heart, liver, spleen, kidney was observed, with the liver presenting the strongest fluorescence, reflecting that the liver functions to clean the blood of foreign objects and harmful substances.

Most recently, our group reported amphiphilic poly(maleic anhydridealt-1-octadecene) stabilized gadolinium (Gd) based CIS/ZnS QDs modified with carbodiimide chemistry for a dual-modality nanoprobe magnetic resonance and optical imaging. This material was also used for specific targeting *via* a folate receptor mediated targeted receptor.[239]

4.4 Drug delivery

The surface chemistry of QDs enables connection of numerous ligands for different functionalities and loading of both hydrophobic and hydrophilic therapeutics. Moreover, their physical and chemical stabilities can lead to long systemic circulation times in the cell. With the utility of various coupling strategies, the QDs can be functionalized by a range of cancer-targeting moieties (*e.g.* aptamers, anti-cancer drugs and folic acids). QD-based drug delivery paths must be capable to carry and release the drug to a specific location. Drug delivery systems may be covalent or noncovalent systems and require specific control of temperature, pH, and biological reactions. Covalent systems involve a covalent linkage between the drug and QD which requires breaking of the bond between the QD and the drug which may restrict the release of the drug. Careful design of this linker can give cleavage under specific conditions (thermal, enzymatic or pH based). Noncovalent drug delivery is any form of drug carrier that does not form a chemical bond, *i.e.* the QDs may encapsulate the drug or form stabilizing pockets. Extensive reports have been made about drug delivery systems using QDs.[204,214,240,241]

Previously our group reported AIS/ZnS QDs, by conjugating with anticancer drug methotrexate, that possesses dual-functionality, for optical imaging and drug delivery.[242] The anticancer drug covalently bonded on the surface of QDs which were effective carriers for the anticancer drug.

4.5 Photo-therapeutic applications

Biological researches has also relied on developing alternative cancer cell treatment modalities that are safe, powerful and cost effective. Near infrared (NIR) light mediated photo-therapeutic methods with QDs, such as PTT and PDT show great advantages including better spatiotemporal selectivity, avoidance of surgery, noninvasive, effective and fast treatment, lower cost and reduced side effects.

PTT is a therapeutic strategy, which involves the NIR photo-absorbers generating hyperthermia for thermal ablation of cancer cells on exposure to NIR laser irradiation. It can eradicate the cancer cell in primary tumors and can be combined with other therapeutic modalities to treat cancer cells.[243,244] Up to now, numerous types of photothermal therapeutics have been adopted including plasmonic nanoparticles,[243,245] transition metal sulfide/oxides,[246–249] organic nanoagents,[250–252] nanocarbons[253] and QDs.[254] On the other hand, PDT involves a photosensitizer which can change triplet oxygen ($^3O_2^{\bullet}$) molecule to reactive oxygen species (such as singlet oxygen, hydroxyl radical, peroxides) on exposure to single wavelength light, which causes the death of nearby malignant cancer cells. A more detailed discussion of PDT is provided in a review reported by Lucky *et al.*[255] Wu *et al.*[254] synthesized CIS/ZnS QDs and used them for PTT and PDT by conjugating with reduced graphene oxide nanosheets and linking by liposomes, which improves the medical therapeutics of these toxic element free I–III–VI band QDs. Ghosh *et al.*[256] synthesized $CuFeS_2$ QDs by substituting the conventional In atom and applied them for PTT. The report shows that Fe can create an intermediate band which is suitable for light-to-heat conversion.

Recently, Lv *et al.*[257] demonstrated the *in vitro* and *in vivo* theranostic applications of CIS/ZnS which combines imaging and therapeutic nanomedicines. Such "all in one" nanomedicines are attractive for particular diagnosis and effective destruction of tumors. Simultaneous PTT and PDT using single wavelength laser irradiation (Fig. 15) leads to application of these materials for effective synergistic phototherapy against tumors with negligible toxicity.

5. Toxicity and biocompatibility

Biocompatibility of QDs is related to the response of the immune system following its administration and intrinsic toxicity due to biodegradation metabolites. In general, most QDs are prepared in organic solvents, and a phase change, surface functionalization and bioconjugation is usually required before applying them for biomedical uses. The cytotoxicity issue is to some degree challenging. The level of toxicity would relate to the intrinsic toxic nature of QDs themselves, size and structure effects, surface modification, solubility, stability of ligands, charge, delivery method and dosage injected, biodegradability, biodistribution, and pharmacokinetics, and should be carefully

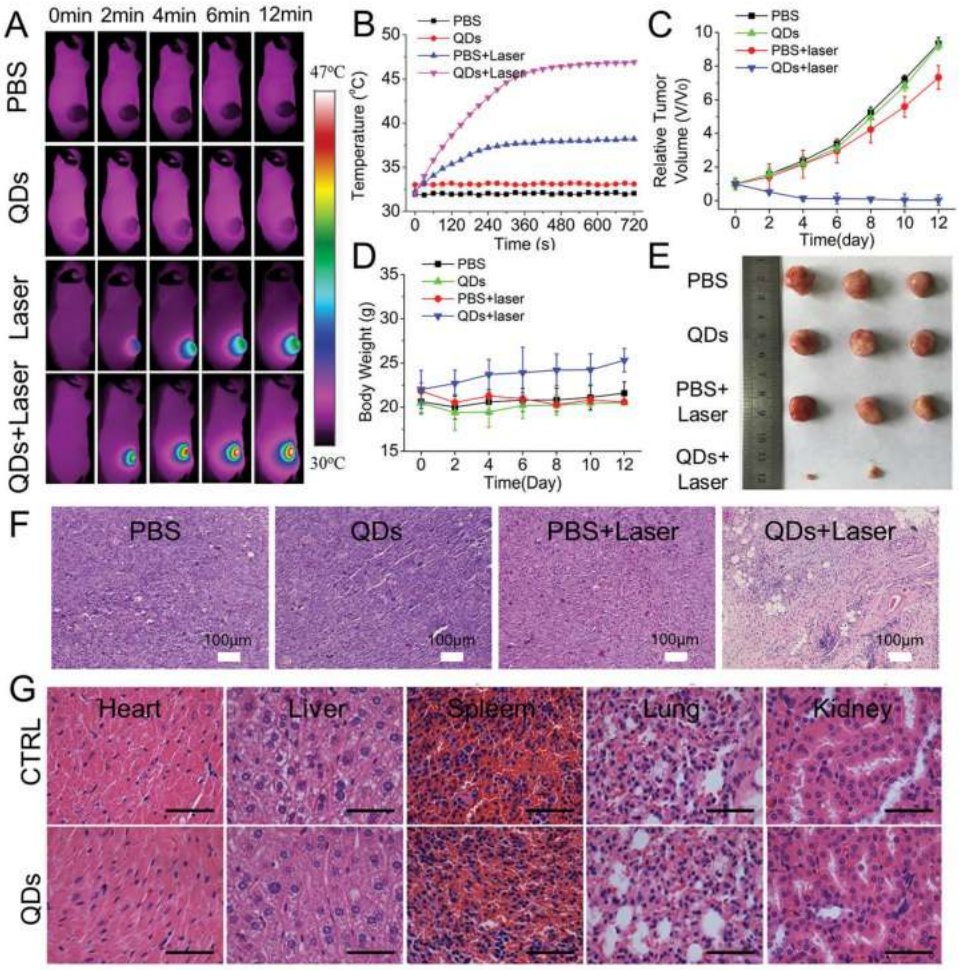

Fig. 15 *In vivo* thermal imaging and PTT. (A) Thermal IR imaging of 4T1 tumor-bearing mice after i.v. injection of ZCIS NMs-25 and exposure to 660 nm laser irradiation. (B) Temperature change curves of 4T1 tumors in mice treated with or without ZCIS NMs-25 and laser irradiation as a function of irradiation time. (C) Growth curves of tumors in mice from the different treatment groups. Tumor volumes were normalized to their initial sizes. Error bars represent the standard deviations of three mice per group. (D) Body weight curves of mice in the different treatment groups. (E) Digital photos and (F) H&E staining of tumor tissues collected from mice in the different groups at the end of treatment. (G) H&E-stained slices of the heart, liver, spleen, lung, and kidney in mice without and with PTT treatment. Scale bar = 50 μm. (Reproduced from ref. 257 with permission from the American Chemical Society.)

considered. Furthermore, QDs must be eliminated from the body in the shortest possible time. Despite all the inspiring progress of QDs, the cytotoxic actions are not entirely clear, since *in vitro* and animal studies are conducted with varied range of QDs concentration, size and structure, surface modifications, exposure time, and delivery methods, *etc.* making it challenging to forecast the cytotoxicity of QDs for new designs.[56,167,214,227,232,239] However, compared to cadmium based QDs, I–III–VI QDs have lower cytotoxicity. Furthermore, their higher PLQY, size tunable photoluminescence, high photo and chemical stability and broad absorption spectra are a further advantage. Wider research should be addressed to eliminate cytotoxicity related issues.

Clearance of QDs from the body is a key factor for clinical application of any *in vivo* diagnosis and therapeutic agents. It was previously reported that smaller QDs (<5 nm) can be removed by renal pathways from the blood which protects QDs accumulation on the cancer cells. QDs of 10–20 nm size can be consumed by the liver, and larger QDs (>200 nm) size are filtered by spleen or reticulo-endothelial system.[258–260] Once the QDs are transported to the cancer cell, they should be spread to the cancer cell, consumed by the cancer cell, and localized intracellularly to execute therapeutic action. Pons *et al.*[73] reported that shell growth and monitored dosage of CIS/ZnS QDs much reduced *in vivo* local acute toxicity. To evaluate the *in vivo* clearance process and biodistribution, adult zebrafish were exposed to a solution of as-prepared Q-dots. For example, Chetty *et al.*[261] studied zebrafish embryos to check the toxicities of CIS/ZnS QDs. As reported up to a minimal dosage it shows minimal toxicity and minimal acute teratogenic consequences. In summary, there is still much work to do

in understanding toxicity concerns in the application of QDs in bioapplications. Study of experimental conditions, dosages, experimental cell lines for *in vitro* studies, and animal models for *in vivo* studies should lead to increasing understanding of toxicity. *In vitro* experiments are valuable to investigate new QDs at the early stages of research for quantitative measurements of toxicity. Whereas, *in vivo* experiments can be used to evaluate neurological, cardiovascular, immunological, reproductive and developmental related toxicity to assess chronic systemic toxicity of QDs.

6. Conclusions and outlook

Bioconjugated QDs are widely used as nanoplatforms for several biomedical applications, such as biosensing, imaging, diagnosis and therapy. Specifically, through careful material composition and engineering with versatile surface molecules for biological conjugation can lead to very advantageous and multifunctional I–III–VI QD-based materials for advanced theranostics. In this review, we discussed recent advances of I–III–VI QDs for various biological applications. QD-based nanoprobes are considered as effective for biosensors, optical imaging, MRI, drug carriers, in therapy and in multimodal nanomedicines. We have discussed the optical properties, synthesis protocols, and surface modification strategies as well as bioconjugation of I–III–VI QDs. The optical properties of I–III–VI QDs display excellent features that are essential for biosensors, imaging, PTT and PDT. For example, tunable photoluminescence, a broad absorption spectra spanning from UV to NIR, higher QY and large Stokes shift are observed. In addition, the availability of various surface chemistries and low toxicity of such QDs leads to novel biomedical applications.

Despite extensive reports of the synthesis of doped ternary systems both in core and shell, the proportion and location of the incoming atom should be carefully considered for novel synthesis methods. Other challenges to be addressed for QD probes are their biocompatibility, targeting efficacy, noninvasiveness and long-term stability, and clinical applications. Pointing to expanding QDs usage even further, early steps have been made to design multifunctional nanomedicines, that promise to combine the advantages of multiple imaging modalities, such as contrast agent together with chemotherapy and phototherapy. Prior to biological application with these I–III–VI QDs, we should reduce the toxicity of these materials by using appropriate surface modification such as biocompatible polymers, DNA/RNA, peptides *etc.* After improving their biocompatibility, in future, research development could focus on the QD-based biomedical imaging, and therapeutic intervention techniques for monitoring and therapy of malignant cells.

Conflict of interest

The authors declare no conflict of interest.

Acknowledgements

This work was supported by the Ministry of Science and Technology of the Republic of China under Contract No. MOST 106-2113-M-011-002.

References

1 J. Zhao, J. A. Bardecker, A. M. Munro, M. S. Liu, Y. Niu, I. K. Ding, J. Luo, B. Chen, A. K. Y. Jen and D. S. Ginger, *Nano Lett.*, 2006, **6**, 463–467.
2 A. Aboulaich, M. Michalska, R. Schneider, A. Potdevin, J. Deschamps, R. Deloncle, G. Chadeyron and R. Mahiou, *ACS Appl. Mater. Interfaces*, 2014, **6**, 252–258.
3 B. Chen, Q. Zhou, J. Li, F. Zhang, R. Liu, H. Zhong and B. Zou, *Opt. Express*, 2013, **21**, 10105–10110.
4 Z. Bai, W. Ji, D. Han, L. Chen, B. Chen, H. Shen, B. Zou and H. Zhong, *Chem. Mater.*, 2016, **28**, 1085–1091.
5 P.-H. Chuang, C. C. Lin and R.-S. Liu, *ACS Appl. Mater. Interfaces*, 2014, **6**, 15379–15387.
6 I. Robel, V. Subramanian, M. Kuno and P. V. Kamat, *J. Am. Chem. Soc.*, 2006, **128**, 2385–2393.
7 I. L. Medintz, H. T. Uyeda, E. R. Goldman and H. Mattoussi, *Nat. Mater.*, 2005, **4**, 435–446.
8 L. Li, T. J. Daou, I. Texier, T. T. Kim Chi, N. Q. Liem and P. Reiss, *Chem. Mater.*, 2009, **21**, 2422–2429.
9 Z. Lin, X. Fei, Q. Ma, X. Gao and X. Su, *New J. Chem.*, 2014, **38**, 90–96.
10 L. Jeong, Yu, N. Dong Heon, O. Mi Hwa, K. Youngsun, C. Hyung Seok, J. Duk Young, P. Chan Beum and N. Yoon Sung, *Nanotechnology*, 2014, **25**, 175702.
11 P. Reiss, M. Protière and L. Li, *Small*, 2009, **5**, 154–168.
12 Z. Chen and S. O'Brien, *ACS Nano*, 2008, **2**, 1219–1229.
13 Y. Gai, H. Peng and J. Li, *J. Phys. Chem. C*, 2009, **113**, 21506–21511.
14 J. Zhou, Y. Yang and C.-Y. Zhang, *Chem. Rev.*, 2015, **115**, 11669–11717.
15 K. D. Wegner and N. Hildebrandt, *Chem. Soc. Rev.*, 2015, **44**, 4792–4834.
16 A. M. Smith, H. Duan, A. M. Mohs and S. Nie, *Adv. Drug Delivery Rev.*, 2008, **60**, 1226–1240.
17 C. M. Tyrakowski and P. T. Snee, *Phys. Chem. Chem. Phys.*, 2014, **16**, 837–855.
18 P. Zrazhevskiy, M. Sena and X. Gao, *Chem. Soc. Rev.*, 2010, **39**, 4326–4354.
19 H. Mattoussi, G. Palui and H. B. Na, *Adv. Drug Delivery Rev.*, 2012, **64**, 138–166.
20 W. R. Algar, M. H. Stewart, A. M. Scott, W. J. Moon and I. L. Medintz, *J. Mater. Chem. B*, 2014, **2**, 7816–7827.
21 J. M. Klostranec and W. C. Chan, *Adv. Mater.*, 2006, **18**, 1953–1964.
22 L. E. Brus, *J. Chem. Phys.*, 1984, **80**, 4403–4409.
23 L. Brus, *J. Phys. Chem.*, 1986, **90**, 2555–2560.
24 A. M. Smith and S. Nie, *Analyst*, 2004, **129**, 672–677.
25 H. Zhong, Z. Bai and B. Zou, *J. Phys. Chem. Lett.*, 2012, **3**, 3167–3175.

26 H. Y. Ueng and H. L. Hwang, *J. Phys. Chem. Solids*, 1989, **50**, 1297–1305.
27 J. E. Jaffe and A. Zunger, *Phys. Rev. B*, 1984, **29**, 1882–1906.
28 J. Shay, B. Tell, L. Schiavone, H. Kasper and F. Thiel, *Phys. Rev. B: Solid State*, 1974, **9**, 1719.
29 K. Koitabashi, S. Ozaki and S. Adachi, *J. Appl. Phys.*, 2010, **107**, 053516.
30 W. Yue, S. Han, R. Peng, W. Shen, H. Geng, F. Wu, S. Tao and M. Wang, *J. Mater. Chem.*, 2010, **20**, 7570–7578.
31 L. Li, A. Pandey, D. J. Werder, B. P. Khanal, J. M. Pietryga and V. I. Klimov, *J. Am. Chem. Soc.*, 2011, **133**, 1176–1179.
32 M. D. Regulacio, K. Y. Win, S. L. Lo, S.-Y. Zhang, X. Zhang, S. Wang, M.-Y. Han and Y. Zheng, *Nanoscale*, 2013, **5**, 2322–2327.
33 D. Deng, L. Qu and Y. Gu, *J. Mater. Chem. C*, 2014, **2**, 7077–7085.
34 X. Kang, Y. Yang, L. Wang, S. Wei and D. Pan, *ACS Appl. Mater. Interfaces*, 2015, **7**, 27713–27719.
35 H. Zhong, Y. Zhou, M. Ye, Y. He, J. Ye, C. He, C. Yang and Y. Li, *Chem. Mater.*, 2008, **20**, 6434–6443.
36 B. Chen, H. Zhong, W. Zhang, Z. A. Tan, Y. Li, C. Yu, T. Zhai, Y. Bando, S. Yang and B. Zou, *Adv. Funct. Mater.*, 2012, **22**, 2081–2088.
37 M. Uehara, K. Watanabe, Y. Tajiri, H. Nakamura and H. Maeda, *J. Chem. Phys.*, 2008, **129**, 134709.
38 M. Dai, S. Ogawa, T. Kameyama, K.-I. Okazaki, A. Kudo, S. Kuwabata, Y. Tsuboi and T. Torimoto, *J. Mater. Chem.*, 2012, **22**, 12851–12858.
39 D. Deng, L. Qu, J. Zhang, Y. Ma and Y. Gu, *ACS Appl. Mater. Interfaces*, 2013, **5**, 10858–10865.
40 D. Deng, L. Qu and Y. Gu, *J. Mater. Chem. C*, 2014, **2**, 7077.
41 J.-Y. Chang, G.-Q. Wang, C.-Y. Cheng, W.-X. Lin and J.-C. Hsu, *J. Mater. Chem.*, 2012, **22**, 10609–10618.
42 D. H. Jara, K. G. Stamplecoskie and P. V. Kamat, *J. Phys. Chem. Lett.*, 2016, **7**, 1452–1459.
43 A. M. Smith, A. M. Mohs and S. Nie, *Nat. Nanotechnol.*, 2009, **4**, 56–63.
44 Q. Zeng, X. Kong, Y. Sun, Y. Zhang, L. Tu, J. Zhao and H. Zhang, *J. Phys. Chem. C*, 2008, **112**, 8587–8593.
45 S. Kim, B. Fisher, H.-J. Eisler and M. Bawendi, *J. Am. Chem. Soc.*, 2003, **125**, 11466–11467.
46 W.-C. Law, K.-T. Yong, I. Roy, H. Ding, R. Hu, W. Zhao and P. N. Prasad, *Small*, 2009, **5**, 1302–1310.
47 H. Zhu, N. Song and T. Lian, *J. Am. Chem. Soc.*, 2010, **132**, 15038–15045.
48 D. V. Talapin, A. L. Rogach, A. Kornowski, M. Haase and H. Weller, *Nano Lett.*, 2001, **1**, 207–211.
49 X. Fang, Y. Bando, G. Shen, C. Ye, U. K. Gautam, P. M. Costa, C. Zhi, C. Tang and D. Golberg, *Adv. Mater.*, 2007, **19**, 2593–2596.
50 R. Xie, M. Rutherford and X. Peng, *J. Am. Chem. Soc.*, 2009, **131**, 5691–5697.
51 V. Bachmann, C. Ronda and A. Meijerink, *Chem. Mater.*, 2009, **21**, 2077–2084.
52 E. S. Speranskaya, C. Sevrin, S. De Saeger, Z. Hens, I. Y. Goryacheva and C. Grandfils, *ACS Appl. Mater. Interfaces*, 2016, **8**, 7613–7622.
53 Y. Chen, S. Li, L. Huang and D. Pan, *Inorg. Chem.*, 2013, **52**, 7819–7821.
54 W. Guo, *Theranostics*, 2013, **3**, 99.
55 X. Tang, W. B. A. Ho and J. M. Xue, *J. Phys. Chem. C*, 2012, **116**, 9769–9773.
56 W. Yang, W. Guo, X. Gong, B. Zhang, S. Wang, N. Chen, W. Yang, Y. Tu, X. Fang and J. Chang, *ACS Appl. Mater. Interfaces*, 2015, **7**, 18759–18768.
57 H. Nakamura, W. Kato, M. Uehara, K. Nose, T. Omata, S. Otsuka-Yao-Matsuo, M. Miyazaki and H. Maeda, *Chem. Mater.*, 2006, **18**, 3330–3335.
58 X. Kang, Y. Yang, L. Huang, Y. Tao, L. Wang and D. Pan, *Green Chem.*, 2015, **17**, 4482–4488.
59 B. Mao, C.-H. Chuang, F. Lu, L. Sang, J. Zhu and C. Burda, *J. Phys. Chem. C*, 2013, **117**, 648–656.
60 D. Che, X. Zhu, H. Wang, Y. Duan, Q. Zhang and Y. Li, *J. Colloid Interface Sci.*, 2016, **463**, 1–7.
61 C. B. Murray, D. J. Norris and M. G. Bawendi, *J. Am. Chem. Soc.*, 1993, **115**, 8706–8715.
62 C. B. Murray, C. R. Kagan and M. G. Bawendi, *Annu. Rev. Mater. Sci.*, 2000, **30**, 545–610.
63 J. Park, J. Joo, S. G. Kwon, Y. Jang and T. Hyeon, *Angew. Chem., Int. Ed.*, 2007, **46**, 4630–4660.
64 D. Pan, L. An, Z. Sun, W. Hou, Y. Yang, Z. Yang and Y. Lu, *J. Am. Chem. Soc.*, 2008, **130**, 5620–5621.
65 R. P. Raffaelle, S. L. Castro, A. F. Hepp and S. G. Bailey, *Progr. Photovolt.: Res. Appl.*, 2002, **10**, 433–439.
66 S. Liu, H. Zhang, Y. Qiao and X. Su, *RSC Adv.*, 2012, **2**, 819–825.
67 S. L. Castro, S. G. Bailey, R. P. Raffaelle, K. K. Banger and A. F. Hepp, *Chem. Mater.*, 2003, **15**, 3142–3147.
68 S. L. Castro, S. G. Bailey, R. P. Raffaelle, K. K. Banger and A. F. Hepp, *J. Phys. Chem. B*, 2004, **108**, 12429–12435.
69 M. G. Panthani, V. Akhavan, B. Goodfellow, J. P. Schmidtke, L. Dunn, A. Dodabalapur, P. F. Barbara and B. A. Korgel, *J. Am. Chem. Soc.*, 2008, **130**, 16770–16777.
70 H. Zhong, S. S. Lo, T. Mirkovic, Y. Li, Y. Ding, Y. Li and G. D. Scholes, *ACS Nano*, 2010, **4**, 5253–5262.
71 A. Lefrançois, S. Pouget, L. Vaure, M. Lopez-Haro and P. Reiss, *ChemPhysChem*, 2016, **17**, 654–659.
72 J. J. Nairn, P. J. Shapiro, B. Twamley, T. Pounds, R. von Wandruszka, T. R. Fletcher, M. Williams, C. Wang and M. G. Norton, *Nano Lett.*, 2006, **6**, 1218–1223.
73 T. Pons, E. Pic, N. Lequeux, E. Cassette, L. Bezdetnaya, F. Guillemin, F. Marchal and B. Dubertret, *ACS Nano*, 2010, **4**, 2531–2538.
74 Y.-K. Kim, S.-H. Ahn, K. Chung, Y.-S. Cho and C.-J. Choi, *J. Mater. Chem.*, 2012, **22**, 1516–1520.
75 Y. Hamanaka, T. Kuzuya, T. Sofue, T. Kino, K. Ito and K. Sumiyama, *Chem. Phys. Lett.*, 2008, **466**, 176–180.
76 D. P. Dutta and G. Sharma, *Mater. Lett.*, 2006, **60**, 2395–2398.
77 J. S. Gardner, E. Shurdha, C. Wang, L. D. Lau, R. G. Rodriguez and J. J. Pak, *J. Nanopart. Res.*, 2008, **10**, 633–641.

78 W. Du, X. Qian, J. Yin and Q. Gong, *Chem.–Eur. J.*, 2007, **13**, 8840–8846.
79 P. M. Allen and M. G. Bawendi, *J. Am. Chem. Soc.*, 2008, **130**, 9240–9241.
80 D. Pan, D. Weng, X. Wang, Q. Xiao, W. Chen, C. Xu, Z. Yang and Y. Lu, *Chem. Commun.*, 2009, 4221–4223.
81 T.-L. Li and H. Teng, *J. Mater. Chem.*, 2010, **20**, 3656–3664.
82 D.-E. Nam, W.-S. Song and H. Yang, *J. Mater. Chem.*, 2011, **21**, 18220.
83 J. Park and S.-W. Kim, *J. Mater. Chem.*, 2011, **21**, 3745.
84 L. Li, A. Pandey, D. J. Werder, B. P. Khanal, J. M. Pietryga and V. I. Klimov, *J. Am. Chem. Soc.*, 2011, **133**, 1176–1179.
85 M. Booth, A. P. Brown, S. D. Evans and K. Critchley, *Chem. Mater.*, 2012, **24**, 2064–2070.
86 L. Liu, R. Hu, W.-C. Law, I. Roy, J. Zhu, L. Ye, S. Hu, X. Zhang and K.-T. Yong, *Analyst*, 2013, **138**, 6144–6153.
87 B. Zhang, Y. Wang, C. Yang, S. Hu, Y. Gao, Y. Zhang, Y. Wang, H. V. Demir, L. Liu and K.-T. Yong, *Phys. Chem. Chem. Phys.*, 2015, **17**, 25133–25141.
88 S. H. Park, A. Hong, J.-H. Kim, H. Yang, K. Lee and H. S. Jang, *ACS Appl. Mater. Interfaces*, 2015, **7**, 6764–6771.
89 A. Arshad, H. Chen, X. Bai, S. Xu and L. Wang, *Chin. J. Chem.*, 2016, **34**, 576–582.
90 M. G. Panthani, C. J. Stolle, D. K. Reid, D. J. Rhee, T. B. Harvey, V. A. Akhavan, Y. Yu and B. A. Korgel, *J. Phys. Chem. Lett.*, 2013, **4**, 2030–2034.
91 H. Zhong, Z. Wang, E. Bovero, Z. Lu, F. C. van Veggel and G. D. Scholes, *J. Phys. Chem. C*, 2011, **115**, 12396–12402.
92 J. Park, C. Dvoracek, K. H. Lee, J. F. Galloway, H. E. C. Bhang, M. G. Pomper and P. C. Searson, *Small*, 2011, **7**, 3148–3152.
93 T. Omata, K. Nose and S. Otsuka-Yao-Matsuo, *J. Nanosci. Nanotechnol.*, 2011, **11**, 4815–4823.
94 O. Yarema, D. Bozyigit, I. Rousseau, L. Nowack, M. Yarema, W. Heiss and V. Wood, *Chem. Mater.*, 2013, **25**, 3753–3757.
95 M. G. Panthani, T. A. Khan, D. K. Reid, D. J. Hellebusch, M. R. Rasch, J. A. Maynard and B. A. Korgel, *Nano Lett.*, 2013, **13**, 4294–4298.
96 E. Cassette, T. Pons, C. Bouet, M. Helle, L. Bezdetnaya, F. Marchal and B. Dubertret, *Chem. Mater.*, 2010, **22**, 6117–6124.
97 X. Liu, G. B. Braun, H. Zhong, D. J. Hall, W. Han, M. Qin, C. Zhao, M. Wang, Z. G. She and C. Cao, *Adv. Funct. Mater.*, 2016, **26**, 267–276.
98 P. M. Allen and M. G. Bawendi, *J. Am. Chem. Soc.*, 2008, **130**, 9240–9241.
99 K. Nose, T. Omata and S. Otsuka-Yao-Matsuo, *J. Phys. Chem. C*, 2009, **113**, 3455–3460.
100 W. Zhou, Z. Yin, D. H. Sim, H. Zhang, J. Ma, H. H. Hng and Q. Yan, *Nanotechnology*, 2011, **22**, 195607.
101 Y. Liao, H. Zhang, Z. Zhong, L. Jia, F. Bai, J. Li, P. Zhong, H. Chen and J. Zhang, *ACS Appl. Mater. Interfaces*, 2013, **5**, 11022–11028.
102 S. Sugan, K. Baskar and R. Dhanasekaran, *Curr. Appl. Phys.*, 2014, **14**, 1416–1420.
103 X. Kang, Y. Yang, L. Huang, Y. Tao, L. Wang and D. Pan, *Green Chem.*, 2015, **17**, 4482–4488.
104 J. Yang, J.-Y. Kim, J. H. Yu, T.-Y. Ahn, H. Lee, T.-S. Choi, Y.-W. Kim, J. Joo, M. J. Ko and T. Hyeon, *Phys. Chem. Chem. Phys.*, 2013, **15**, 20517–20525.
105 W. Li, Z. Pan and X. Zhong, *J. Mater. Chem. A*, 2015, **3**, 1649–1655.
106 V. K. LaMer and R. H. Dinegar, *J. Am. Chem. Soc.*, 1950, **72**, 4847–4854.
107 M. A. Hines and P. Guyot-Sionnest, *J. Phys. Chem. B*, 1998, **102**, 3655–3657.
108 L. S. Li, N. Pradhan, Y. Wang and X. Peng, *Nano Lett.*, 2004, **4**, 2261–2264.
109 M. A. Hines and G. D. Scholes, *Adv. Mater.*, 2003, **15**, 1844–1849.
110 A. Lipovskii, E. Kolobkova, V. Petrikov, I. Kang, A. Olkhovets, T. Krauss, M. Thomas, J. Silcox, F. Wise and Q. Shen, *Appl. Phys. Lett.*, 1997, **71**, 3406–3408.
111 J. M. Pietryga, R. D. Schaller, D. Werder, M. H. Stewart, V. I. Klimov and J. A. Hollingsworth, *J.Am. Chem. Soc.*, 2004, **126**, 11752–11753.
112 W. Lu, J. Fang, K. L. Stokes and J. Lin, *J. Am. Chem. Soc.*, 2004, **126**, 11798–11799.
113 J. J. Urban, D. V. Talapin, E. V. Shevchenko and C. B. Murray, *J. Am. Chem. Soc.*, 2006, **128**, 3248–3255.
114 R. Xie, M. Rutherford and X. Peng, *J. Am. Chem. Soc.*, 2009, **131**, 5691–5697.
115 J. Park and S.-W. Kim, *J. Mater. Chem.*, 2011, **21**, 3745–3750.
116 H. Kim, J. Y. Han, D. S. Kang, S. W. Kim, D. S. Jang, M. Suh, A. Kirakosyan and D. Y. Jeon, *J. Cryst. Growth*, 2011, **326**, 90–93.
117 J. Park and S.-W. Kim, *J. Mater. Chem.*, 2011, **21**, 3745–3750.
118 J. Park, C. Dvoracek, K. H. Lee, J. F. Galloway, H.-E. C. Bhang, M. G. Pomper and P. C. Searson, *Small*, 2011, **7**, 3148–3152.
119 W. Xiang, C. Xie, J. Wang, J. Zhong, X. Liang, H. Yang, L. Luo and Z. Chen, *J. Alloys Compd.*, 2014, **588**, 114–121.
120 T. Torimoto, S. Ogawa, T. Adachi, T. Kameyama, K. Okazaki, T. Shibayama, A. Kudo and S. Kuwabata, *Chem. Commun.*, 2010, **46**, 2082–2084.
121 J.-Y. Chang, G.-Q. Wang, C.-Y. Cheng, W.-X. Lin and J.-C. Hsu, *J. Mater. Chem.*, 2012, **22**, 10609–10618.
122 Y. C. Cao and J. Wang, *J. Am. Chem. Soc.*, 2004, **126**, 14336–14337.
123 C. Xia, L. Cao, W. Liu, G. Su, R. Gao, H. Qu, L. Shi and G. He, *CrystEngComm*, 2014, **16**, 7469–7477.
124 W. Zhang and X. Zhong, *Inorg. Chem.*, 2011, **50**, 4065–4072.
125 M. Dai, S. Ogawa, T. Kameyama, K.-I. Okazaki, A. Kudo, S. Kuwabata, Y. Tsuboi and T. Torimoto, *J. Mater. Chem.*, 2012, **22**, 12851.
126 T. Kameyama, Y. Douke, H. Shibakawa, M. Kawaraya, H. Segawa, S. Kuwabata and T. Torimoto, *J. Phys. Chem. C*, 2014, **118**, 29517–29524.
127 R. I. Walton, *Chem. Soc. Rev.*, 2002, **31**, 230–238.
128 H. Chen, S.-M. Yu, D.-W. Shin and J.-B. Yoo, *Nanoscale Res. Lett.*, 2010, **5**, 217–223.
129 W.-C. Huang, C.-H. Tseng, S.-H. Chang, H.-Y. Tuan, C.-C. Chiang, L.-M. Lyu and M. H. Huang, *Langmuir*, 2012, **28**, 8496–8501.

130 K.-C. Cheng, W.-C. Law, K.-T. Yong, J. S. Nevins, D. F. Watson, H.-P. Ho and P. N. Prasad, *Chem. Phys. Lett.*, 2011, **515**, 254–257.
131 X. Tang, K. Yu, Q. Xu, E. S. G. Choo, G. K. L. Goh and J. Xue, *J. Mater. Chem.*, 2011, **21**, 11239.
132 W. Chung, H. Jung, C. H. Lee and S. H. Kim, *J. Mater. Chem. C*, 2014, **2**, 4227.
133 L. Tian, M. T. Ng, N. Venkatram, W. Ji and J. J. Vittal, *Cryst. Growth Des.*, 2010, **10**, 1237–1242.
134 D. Yao, H. Liu, Y. Liu, C. Dong, K. Zhang, Y. Sheng, J. Cui, H. Zhang and B. Yang, *Nanoscale*, 2015, **7**, 18570–18578.
135 H. C. Yoon, J. H. Oh, M. Ko, H. Yoo and Y. R. Do, *ACS Appl. Mater. Interfaces*, 2015, **7**, 7342–7350.
136 Y. Hamanaka, T. Ogawa, M. Tsuzuki and T. Kuzuya, *J. Phys. Chem. C*, 2011, **115**, 1786–1792.
137 M. Z. Fahmi and J. Y. Chang, *Nanoscale*, 2013, **5**, 1517–1528.
138 D.-E. Nam, W.-S. Song and H. Yang, *J. Mater. Chem.*, 2011, **21**, 18220–18226.
139 W.-W. Xiong, G.-H. Yang, X.-C. Wu and J.-J. Zhu, *ACS Appl. Mater. Interfaces*, 2013, **5**, 8210–8216.
140 X. Gao, Z. Liu, Z. Lin and X. Su, *Analyst*, 2014, **139**, 831–836.
141 J. Weng, X. Song, L. Li, H. Qian, K. Chen, X. Xu, C. Cao and J. Ren, *Talanta*, 2006, **70**, 397–402.
142 C. Wang, X. Gao and X. Su, *Anal. Bioanal. Chem.*, 2010, **397**, 1397–1415.
143 A. L. Rogach, L. Katsikas, A. Kornowski, D. Su, A. Eychmüller and H. Weller, *Ber. Bunsen-Ges. Phys. Chem.*, 1996, **100**, 1772–1778.
144 Z. Luo, H. Zhang, J. Huang and X. Zhong, *J. Colloid Interface Sci.*, 2012, **377**, 27–33.
145 P. Subramaniam, S. J. Lee, S. Shah, S. Patel, V. Starovoytov and K. B. Lee, *Adv. Mater.*, 2012, **24**, 4014–4019.
146 M. D. Regulacio, K. Y. Win, S. L. Lo, S. Y. Zhang, X. Zhang, S. Wang, M. Y. Han and Y. Zheng, *Nanoscale*, 2013, **5**, 2322–2327.
147 D. Deng, J. Cao, L. Qu, S. Achilefu and Y. Gu, *Phys. Chem. Chem. Phys.*, 2013, **15**, 5078–5083.
148 J. Song, T. Jiang, T. Guo, L. Liu, H. Wang, T. Xia, W. Zhang, X. Ye, M. Yang, L. Zhu, R. Xia and X. Xu, *Inorg. Chem.*, 2015, **54**, 1627–1633.
149 C. Wang, S. Xu, Y. Shao, Z. Wang, Q. Xu and Y. Cui, *J. Mater. Chem. C*, 2014, **2**, 5111.
150 M. Mousavi-Kamazani and M. Salavati-Niasari, *Composites, Part B*, 2014, **56**, 490–496.
151 W. Zhang, D. Li, Z. Chen, M. Sun, W. Li, Q. Lin and X. Fu, *Mater. Res. Bull.*, 2011, **46**, 975–982.
152 W.-W. Xiong, G.-H. Yang, X.-C. Wu and J.-J. Zhu, *J. Mater. Chem. B*, 2013, **1**, 4160.
153 L. Liu, R. Hu, W. C. Law, I. Roy, J. Zhu, L. Ye, S. Hu, X. Zhang and K. T. Yong, *Analyst*, 2013, **138**, 6144–6153.
154 K.-T. Yong, I. Roy, R. Hu, H. Ding, H. Cai, J. Zhu, X. Zhang, E. J. Bergey and P. N. Prasad, *Integr. Biol.*, 2010, **2**, 121–129.
155 T. Ogawa, T. Kuzuya, Y. Hamanaka and K. Sumiyama, *J. Mater. Chem.*, 2010, **20**, 2226.
156 T. Torimoto, T. Adachi, K.-I. Okazaki, M. Sakuraoka, T. Shibayama, B. Ohtani, A. Kudo and S. Kuwabata, *J. Am. Chem. Soc.*, 2007, **129**, 12388–12389.
157 T. Sasamura, K.-i. Okazaki, A. Kudo, S. Kuwabata and T. Torimoto, *RSC Adv.*, 2012, **2**, 552–559.
158 D. Che, X. Zhu, H. Wang, Y. Duan, Q. Zhang and Y. Li, *J. Colloid Interface Sci.*, 2016, **463**, 1–7.
159 J. Wang, R. Zhang, F. Bao, Z. Han, Y. Gu and D. Deng, *RSC Adv.*, 2015, **5**, 88583–88589.
160 M.-A. Langevin, A. M. Ritcey and C. N. Allen, *ACS Nano*, 2014, **8**, 3476–3482.
161 S. Xu, C. Wang, Q. Sun, Z. Wang and Y. Cui, *Mater. Res. Express*, 2014, **1**, 015020.
162 J. S. Gardner, E. Shurdha, C. Wang, L. D. Lau, R. G. Rodriguez and J. J. Pak, *J. Nanopart. Res.*, 2008, **10**, 633–641.
163 C.-C. Wu, C.-Y. Shiau, D. W. Ayele, W.-N. Su, M.-Y. Cheng, C.-Y. Chiu and B.-J. Hwang, *Chem. Mater.*, 2010, **22**, 4185–4190.
164 R. Hoogenboom and U. S. Schubert, *Macromol. Rapid Commun.*, 2007, **28**, 368–386.
165 H. Bux, F. Liang, Y. Li, J. Cravillon, M. Wiebcke and J. R. Caro, *J. Am. Chem. Soc.*, 2009, **131**, 16000–16001.
166 J. M. Collins and N. E. Leadbeater, *Org. Biomol. Chem.*, 2007, **5**, 1141–1150.
167 J.-Y. Chang, G.-R. Chen and J.-D. Li, *Phys. Chem. Chem. Phys.*, 2016, **18**, 7132–7140.
168 T. Jamieson, R. Bakhshi, D. Petrova, R. Pocock, M. Imani and A. M. Seifalian, *Biomaterials*, 2007, **28**, 4717–4732.
169 Z. Luo, H. Zhang, J. Huang and X. Zhong, *J. Colloid Interface Sci.*, 2012, **377**, 27–33.
170 C. Zhao, Z. Bai, X. Liu, Y. Zhang, B. Zou and H. Zhong, *ACS Appl. Mater. Interfaces*, 2015, **7**, 17623–17629.
171 D. M. Willard, L. L. Carillo, J. Jung and A. Van Orden, *Nano Lett.*, 2001, **1**, 469–474.
172 H. Mattoussi, J. M. Mauro, E. R. Goldman, G. P. Anderson, V. C. Sundar, F. V. Mikulec and M. G. Bawendi, *J. Am. Chem. Soc.*, 2000, **122**, 12142–12150.
173 G. P. Mitchell, C. A. Mirkin and R. L. Letsinger, *J. Am. Chem. Soc.*, 1999, **121**, 8122–8123.
174 R. Hong, N. O. Fischer, A. Verma, C. M. Goodman, T. Emrick and V. M. Rotello, *J. Am. Chem. Soc.*, 2004, **126**, 739–743.
175 A. R. Clapp, I. L. Medintz and H. Mattoussi, *ChemPhysChem*, 2006, **7**, 47–57.
176 K. E. Sapsford, L. Berti and I. L. Medintz, *Angew. Chem., Int. Ed.*, 2006, **45**, 4562–4589.
177 A. R. Clapp, E. R. Goldman and H. Mattoussi, *Nat. Protoc.*, 2006, **1**, 1258–1266.
178 J. K. Jaiswal, E. R. Goldman, H. Mattoussi and S. M. Simon, *Nat. Methods*, 2004, **1**, 73–78.
179 W. Liu, H. S. Choi, J. P. Zimmer, E. Tanaka, J. V. Frangioni and M. Bawendi, *J. Am. Chem. Soc.*, 2007, **129**, 14530–14531.
180 H. T. Uyeda, I. L. Medintz, J. K. Jaiswal, S. M. Simon and H. Mattoussi, *J. Am. Chem. Soc.*, 2005, **127**, 3870–3878.
181 K. Susumu, H. T. Uyeda, I. L. Medintz, T. Pons, J. B. Delehanty and H. Mattoussi, *J. Am. Chem. Soc.*, 2007, **129**, 13987–13996.

182 T. Pons, H. T. Uyeda, I. L. Medintz and H. Mattoussi, *J. Phys. Chem. B*, 2006, **110**, 20308–20316.
183 J. P. Zimmer, S.-W. Kim, S. Ohnishi, E. Tanaka, J. V. Frangioni and M. G. Bawendi, *J. Am. Chem. Soc.*, 2006, **128**, 2526–2527.
184 W. Liu, M. Howarth, A. B. Greytak, Y. Zheng, D. G. Nocera, A. Y. Ting and M. G. Bawendi, *J. Am. Chem. Soc.*, 2008, **130**, 1274–1284.
185 P. Subramaniam, S. J. Lee, S. Shah, S. Patel, V. Starovoytov and K.-B. Lee, *Adv. Mater.*, 2012, **24**, 4014–4019.
186 Y. Chen, R. Thakar and P. T. Snee, *J. Am. Chem. Soc.*, 2008, **130**, 3744–3745.
187 X. Gao, Y. Cui, R. M. Levenson, L. W. K. Chung and S. Nie, *Nat. Biotechnol.*, 2004, **22**, 969–976.
188 I. Geissbuehler, R. Hovius, K. L. Martinez, M. Adrian, K. R. Thampi and H. Vogel, *Angew. Chem., Int. Ed.*, 2005, **44**, 1388–1392.
189 O. Carion, B. Mahler, T. Pons and B. Dubertret, *Nat. Protoc.*, 2007, **2**, 2383–2390.
190 D. Gerion, F. Pinaud, S. C. Williams, W. J. Parak, D. Zanchet, S. Weiss and A. P. Alivisatos, *J. Phys. Chem. B*, 2001, **105**, 8861–8871.
191 W. Guo, J. J. Li, Y. A. Wang and X. Peng, *Chem. Mater.*, 2003, **15**, 3125–3133.
192 F. Osaki, T. Kanamori, S. Sando, T. Sera and Y. Aoyama, *J. Am. Chem. Soc.*, 2004, **126**, 6520–6521.
193 T. Pellegrino, L. Manna, S. Kudera, T. Liedl, D. Koktysh, A. L. Rogach, S. Keller, J. Rädler, G. Natile and W. J. Parak, *Nano Lett.*, 2004, **4**, 703–707.
194 E. S. Speranskaya, C. Sevrin, S. De Saeger, Z. Hens, I. Goryacheva and C. Grandfils, *ACS Appl. Mater. Interfaces*, 2016, **8**, 7613–7622.
195 M. D. Regulacio, K. Y. Win, S. L. Lo, S.-Y. Zhang, X. Zhang, S. Wang, M.-Y. Han and Y. Zheng, *Nanoscale*, 2013, **5**, 2322–2327.
196 S. Kim and M. G. Bawendi, *J. Am. Chem. Soc.*, 2003, **125**, 14652–14653.
197 J. M. Slocik, J. T. Moore and D. W. Wright, *Nano Lett.*, 2002, **2**, 169–173.
198 F. Pinaud, D. King, H.-P. Moore and S. Weiss, *J. Am. Chem. Soc.*, 2004, **126**, 6115–6123.
199 M. Z. Fahmi and J.-Y. Chang, *Nanoscale*, 2013, **5**, 1517–1528.
200 X. Tang, K. Yu, Q. Xu, E. S. G. Choo, G. K. L. Goh and J. Xue, *J. Mater. Chem.*, 2011, **21**, 11239–11243.
201 D. Deng, L. Qu, J. Zhang, Y. Ma and Y. Gu, *ACS Appl. Mater. Interfaces*, 2013, **5**, 10858–10865.
202 M. F. Foda, L. Huang, F. Shao and H.-Y. Han, *ACS Appl. Mater. Interfaces*, 2014, **6**, 2011–2017.
203 Y. Sheng, X. Tang and J. Xue, *J. Mater. Chem.*, 2012, **22**, 1290–1296.
204 M. Z. Fahmi, K.-L. Ou, J.-K. Chen, M.-H. Ho, S.-H. Tzing and J.-Y. Chang, *RSC Adv.*, 2014, **4**, 32762–32772.
205 N. Erathodiyil and J. Y. Ying, *Acc. Chem. Res.*, 2011, **44**, 925–935.
206 P. Reiss, M. Carrière, C. Lincheneau, L. Vaure and S. Tamang, *Chem. Rev.*, 2016, **116**, 10731–10819.
207 J. Hühn, C. Carrillo-Carrion, M. G. Soliman, C. Pfeiffer, D. Valdeperez, A. Masood, I. Chakraborty, L. Zhu, M. Gallego and Z. Yue, *Chem. Mater.*, 2016, **29**, 399–461.
208 K. E. Knowles, K. H. Hartstein, T. B. Kilburn, A. Marchioro, H. D. Nelson, P. J. Whitham and D. R. Gamelin, *Chem. Rev.*, 2016, **116**, 10820–10851.
209 N. Hildebrandt, C. M. Spillmann, W. R. Algar, T. Pons, M. H. Stewart, E. Oh, K. Susumu, S. A. Díaz, J. B. Delehanty and I. L. Medintz, *Chem. Rev.*, 2017, **117**, 536–711.
210 L. Jing, S. V. Kershaw, Y. Li, X. Huang, Y. Li, A. L. Rogach and M. Gao, *Chem. Rev.*, 2016, **116**, 10623–10730.
211 G. Xu, S. Zeng, B. Zhang, M. T. Swihart, K.-T. Yong and P. N. Prasad, *Chem. Rev.*, 2016, **116**, 12234–12327.
212 G. Xu, S. Mahajan, I. Roy and K.-T. Yong, *Front. Pharmacol.*, 2013, **4**, 140.
213 P. Wu and X.-P. Yan, *Chem. Soc. Rev.*, 2013, **42**, 5489–5521.
214 J.-C. Hsu, C.-C. Huang, K.-L. Ou, N. Lu, F.-D. Mai, J.-K. Chen and J.-Y. Chang, *J. Mater. Chem.*, 2011, **21**, 19257–19266.
215 S. Mazumder, R. Dey, M. Mitra, S. Mukherjee and G. Das, *J. Nanomater.*, 2009, **2009**, 38.
216 J. Gao, H. Gu and B. Xu, *Acc. Chem. Res.*, 2009, **42**, 1097–1107.
217 Y. Wang, R. Hu, G. Lin, I. Roy and K.-T. Yong, *ACS Appl. Mater. Interfaces*, 2013, **5**, 2786–2799.
218 S. Silvi and A. Credi, *Chem. Soc. Rev.*, 2015, **44**, 4275–4289.
219 X. Gao, X. Liu, Z. Lin, S. Liu and X. Su, *Analyst*, 2012, **137**, 5620–5624.
220 E. S. Speranskaya, N. V. Beloglazova, S. Abé, T. Aubert, P. F. Smet, D. Poelman, I. Y. Goryacheva, S. De Saeger and Z. Hens, *Langmuir*, 2014, **30**, 7567–7575.
221 L. Wang, X. Kang and D. Pan, *Inorg. Chem.*, 2017, **56**, 6122–6130.
222 G. Gaur, D. S. Koktysh and S. M. Weiss, *Adv. Funct. Mater.*, 2013, **23**, 3604–3614.
223 A. Crut, B. Geron-Landre, I. Bonnet, S. Bonneau, P. Desbiolles and C. Escudé, *Nucleic Acids Res.*, 2005, **33**, e98–e98.
224 D. Deng, L. Qu and Y. Gu, *J. Mater. Chem. C*, 2014, **2**, 7077–7085.
225 M. Wang, X. Liu, C. Cao and L. Wang, *J. Mater. Chem.*, 2012, **22**, 21979–21986.
226 J. Y. Lee, D. H. Nam, M. H. Oh, Y. Kim, H. S. Choi, D. Y. Jeon, C. B. Park and Y. S. Nam, *Nanotechnology*, 2014, **25**, 175702.
227 W. Guo, N. Chen, C. Dong, Y. Tu, J. Chang and B. Zhang, *RSC Adv.*, 2013, **3**, 9470–9475.
228 J. Song, C. Ma, W. Zhang, X. Li, W. Zhang, R. Wu, X. Cheng, A. Ali, M. Yang and L. Zhu, *ACS Appl. Mater. Interfaces*, 2016, **8**, 24826–24836.
229 H. S. Choi, Y. Kim, J. C. Park, M. H. Oh, D. Y. Jeon and Y. S. Nam, *RSC Adv.*, 2015, **5**, 43449–43455.
230 P. Caravan, J. J. Ellison, T. J. McMurry and R. B. Lauffer, *Chem. Rev.*, 1999, **99**, 2293–2352.
231 M. Kueny-Stotz, A. Garofalo and D. Felder-Flesch, *Eur. J. Inorg. Chem.*, 2012, 1987–2005.

232 P.-Y. Lai, C.-C. Huang, T.-H. Chou, K.-L. Ou and J.-Y. Chang, *Acta Biomater.*, 2017, **50**, 522–533.
233 R. Qiao, C. Yang and M. Gao, *J. Mater. Chem.*, 2009, **19**, 6274–6293.
234 L. Jing, K. Ding, S. V. Kershaw, I. M. Kempson, A. L. Rogach and M. Gao, *Adv. Mater.*, 2014, **26**, 6367–6386.
235 F. Hu and Y. S. Zhao, *Nanoscale*, 2012, **4**, 6235–6243.
236 B. Lin, X. Yao, Y. Zhu, J. Shen, X. Yang, H. Jiang and X. Zhang, *New J. Chem.*, 2013, **37**, 3076–3083.
237 J. Shen, Y. Li, Y. Zhu, X. Yang, X. Yao, J. Li, G. Huang and C. Li, *J. Mater. Chem. B*, 2015, **3**, 2873–2882.
238 K. Ding, L. Jing, C. Liu, Y. Hou and M. Gao, *Biomaterials*, 2014, **35**, 1608–1617.
239 C.-Y. Cheng, K.-L. Ou, W.-T. Huang, J.-K. Chen, J.-Y. Chang and C.-H. Yang, *ACS Appl. Mater. Interfaces*, 2013, **5**, 4389–4400.
240 P. Zhao, J. Zhang, Y. Zhu, X. Yang, X. Jiang, Y. Yuan, C. Liu and C. Li, *J. Mater. Chem. B*, 2014, **2**, 8372–8377.
241 X. Bai, S. Wang, S. Xu and L. Wang, *TrAC, Trends Anal. Chem.*, 2015, **73**, 54–63.
242 P.-J. Wu, K.-L. Ou, J.-K. Chen, H.-P. Fang, S.-H. Tzing, W.-X. Lin and J.-Y. Chang, *Mater. Lett.*, 2014, **128**, 412–416.
243 A. Kumar, S. Kumar, W.-K. Rhim, G.-H. Kim and J.-M. Nam, *J. Am. Chem. Soc.*, 2014, **136**, 16317–16325.
244 J. Lin, M. Wang, H. Hu, X. Yang, B. Wen, Z. Wang, O. Jacobson, J. Song, G. Zhang and G. Niu, *Adv. Mater.*, 2016, **28**, 3273–3279.
245 S. Wang, A. Riedinger, H. Li, C. Fu, H. Liu, L. Li, T. Liu, L. Tan, M. J. Barthel and G. Pugliese, *ACS Nano*, 2015, **9**, 1788–1800.
246 Y. Li, W. Lu, Q. Huang, C. Li and W. Chen, *Nanomedicine*, 2010, **5**, 1161–1171.
247 T. A. Larson, J. Bankson, J. Aaron and K. Sokolov, *Nanotechnology*, 2007, **18**, 325101.
248 J. Liu, X. Zheng, L. Yan, L. Zhou, G. Tian, W. Yin, L. Wang, Y. Liu, Z. Hu, Z. Gu, C. Chen and Y. Zhao, *ACS Nano*, 2015, **9**, 696–707.
249 Y. Yong, X. Cheng, T. Bao, M. Zu, L. Yan, W. Yin, C. Ge, D. Wang, Z. Gu and Y. Zhao, *ACS Nano*, 2015, **9**, 12451–12463.
250 K. Yang, H. Xu, L. Cheng, C. Sun, J. Wang and Z. Liu, *Adv. Mater.*, 2012, **24**, 5586–5592.
251 L. Cheng, W. He, H. Gong, C. Wang, Q. Chen, Z. Cheng and Z. Liu, *Adv. Funct. Mater.*, 2013, **23**, 5893–5902.
252 Y. Yang, J. Liu, C. Liang, L. Feng, T. Fu, Z. Dong, Y. Chao, Y. Li, G. Lu and M. Chen, *ACS Nano*, 2016, **10**, 2774–2781.
253 Z. Liu and X.-J. Liang, *Theranostics*, 2012, **2**, 235–237.
254 Q. Wu, M. Chu, Y. Shao, F. Wo and D. Shi, *Carbon*, 2016, **108**, 21–37.
255 S. S. Lucky, K. C. Soo and Y. Zhang, *Chem. Rev.*, 2015, **115**, 1990–2042.
256 S. Ghosh, T. Avellini, A. Petrelli, I. Kriegel, R. Gaspari, G. Almeida, G. Bertoni, A. Cavalli, F. Scotognella and T. Pellegrino, *Chem. Mater.*, 2016, **28**, 4848–4858.
257 G. Lv, W. Guo, W. Zhang, T. Zhang, S. Li, S. Chen, A. S. Eltahan, D. Wang, Y. Wang and J. Zhang, *ACS Nano*, 2016, **10**, 9637–9645.
258 C. Alric, I. Miladi, D. Kryza, J. Taleb, F. Lux, R. Bazzi, C. Billotey, M. Janier, P. Perriat and S. Roux, *Nanoscale*, 2013, **5**, 5930–5939.
259 J. Liu, M. Yu, C. Zhou, S. Yang, X. Ning and J. Zheng, *J. Am. Chem. Soc.*, 2013, **135**, 4978–4981.
260 A. Gautam and F. C. van Veggel, *J. Mater. Chem. B*, 2013, **1**, 5186–5200.
261 S. S. Chetty, S. Praneetha, S. Basu, C. Sachidanandan and A. V. Murugan, *Sci. Rep.*, 2016, **6**, 26078.

HASIL CEK_60201248 JURNAL 2

ORIGINALITY REPORT

94%	92%	92%	15%
SIMILARITY INDEX	INTERNET SOURCES	PUBLICATIONS	STUDENT PAPERS

PRIMARY SOURCES

1	pubs.rsc.org Internet Source	45%
2	Wubshet Mekonnen Girma, Mochamad Zakki Fahmi, Adi Permadi, Mulu Alemayehu Abate, Jia-Yaw Chang. "Synthetic strategies and biomedical applications of I–III–VI ternary quantum dots", Journal of Materials Chemistry B, 2017 Publication	44%
3	Submitted to University of North Texas Student Paper	2%
4	dro.deakin.edu.au Internet Source	1%
5	Submitted to Xiamen University Student Paper	1%
6	etheses.whiterose.ac.uk Internet Source	<1%
7	Submitted to University of Birmingham Student Paper	<1%

8	Bujak, Piotr. "Core and surface engineering in binary, ternary and quaternary semiconductor nanocrystals﷽A critical review", Synthetic Metals, 2016. Publication	<1%
9	Joanna Kolny-Olesiak, Horst Weller. " Synthesis and Application of Colloidal CuInS Semiconductor Nanocrystals ", ACS Applied Materials & Interfaces, 2013 Publication	<1%

Exclude quotes	On	Exclude matches	Off
Exclude bibliography	On		